RHEL/R 262
Rutherford Laboratory
Report

A Survey of Position Sensitive Detectors and Multi-Counter Arrays with Particular Reference to Thermal Neutron Scattering

B H Meardon D C Salter

Science Research Council

Neutron Beam Research Unit
Rutherford High Energy Laboratory
Chilton Didcot Berkshire
1972

SBN 90237648 9

Available from HMSO
price 80p net

RHEL/R 262

NBRU/72-7

SCIENCE RESEARCH COUNCIL

A SURVEY OF POSITION SENSITIVE DETECTORS AND MULTI-COUNTER ARRAYS WITH PARTICULAR REFERENCE TO THERMAL NEUTRON SCATTERING

B H Meardon and D C Salter

ABSTRACT

Position sensitive detectors have not, so far, been used for thermal neutron studies in the United Kingdom. This report is a survey of position sensitive detection systems and multi-counter arrays with the aim of indicating their potential for use and development in this field. Fundamental aspects of thermal neutron detection and scattering are discussed. Particular detection systems are considered for the many branches of study and recommendations are made.

Neutron Beam Research Unit
Rutherford High Energy Laboratory
Chilton Didcot Berkshire

November 1972

CONTENTS

1 INTRODUCTION

At the meeting of the Neutron Beam Research Committee held on 2 September 1971 the Neutron Beam Research Unit was asked to conduct a 'state of the art' survey of position sensitive detectors and multi-counter arrays. The present memorandum is a result of this survey. In order to correlate the many aspects of position sensitive detectors (PSD) and multi-counter arrays to the requirements imposed by thermal neutron scattering studies it has been necessary to extend the report to include some of the more fundamental aspects of neutron detection.

A position sensitive detector is one that enables the position of a detected particle to be defined over an extended area. Such devices may be used in thermal neutron studies to measure the scattering from a sample in either one or two dimensions. There is in principle no difference between a high density multi-counter array and a PSD; the multi-counter array effectively being a digital PSD.

The obvious advantage of a PSD or large multi-counter array is that it can count simultaneously over a large solid angle. There are, however, three main disadvantages:

(i) The background intensity is integrated over the area of the detector requiring higher counting rates to be handled.

(ii) Collimation cannot be placed in front of large area detectors to reduce background and to extend the useful sample size for a given resolution.

(iii) In general PSD's require the use of a small on-line computer to calculate and store the positional information for each detected particle.

In many instances these disadvantages can be outweighed by the large saving in counting time that may be achieved by using a PSD as opposed to single stepping detectors.

PSD systems have been extensively used over the past 10 years for measuring the co-ordinates of high energy particles. Here the energies involved are many orders of magnitude greater than those associated with thermal neutrons and the majority of devices have been used with charged particles. Until 1967 no position sensitive detectors had been developed for the detection of slow neutrons. Since this date linear one dimensional PSD's have been constructed[1,2,3] and commissioned for thermal neutron detection. Recent advances in France have enabled two dimensional detectors[4,5,6] to be made for special applications; however these will not always be applicable to every requirement. In this survey we have endeavoured to review the fields in which thermal neutrons are at present used, the means by which these low energy uncharged particles may be effectively detected, current and possible PSD systems and their application to specific neutron scattering problems, outlining their advantages and disadvantages. Inevitably in a report of this nature personal preferences tend to emerge. We have tried to minimise these by consultations with others who have given valuable information concerning individual instruments and their requirements.

The Neutron Beam Research Committee operate a rental agreement between the SRC and the UKAEA for the provision of neutron facilities for University scientists on the HERALD, DIDO and PLUTO reactors and the Harwell LINAC. Appendix II shows the current detector systems in use on these facilities and demonstrates how little work has been done on PSD's in this country. We hope that this memorandum will assist towards future development of position sensitive detectors for thermal neutron scattering in the UK.

2 THERMAL NEUTRON SCATTERING

Thermal neutrons of energy 0.4 - 10^{-4} eV which have the associated wavelengths shown in Fig. 1 are extensively used for the study of condensed matter[7,8,9,10,11,12]. The two methods used for the production of thermal neutrons are reactor fission and pulsed high energy electron bombardment of a high atomic number target (LINAC). In this latter case γ rays are produced

which are then absorbed, often in the same target, to give (γ,n) reactions. The fast neutrons emitted in each case are moderated, and channelled to the experimental apparatus along beam tubes which can contain filters and fine collimators. The resulting spectrum obtained at the experiment is characteristic of the moderator temperature at the source end of the beam tube. For an ambient moderator the spectrum obtained from a reactor and linac are shown in Fig. 2. Due to the incomplete thermalisation in the case of the linac moderator the flux is relatively higher for shorter wavelengths than in the case of the reactor where thermalisation is virtually complete. Thus the linac system is more suited for those studies requiring higher incident energies.

A higher energy spectrum may also be produced in a reactor by heating the small portion of the moderator viewed by the beam tube. This 'hot source' increases the effective neutron temperature within the source and so shifts the spectrum emerging from the beam hole to higher energies. For experiments requiring a higher flux at lower energies a cold source is used. This cools a portion of the moderator, typically to $20^{o}K$, which moves the spectrum peak to approx. 4 Å.

Many of the calculations in this report have been made at 1Å as this is approximately a mean peak wavelength in thermal neutron studies. In general the effect of working with longer wavelengths will result in an increase in the detection efficiency but accompanying this will be an increase in the neutron absorption by the walls of any containment vessel. Conversely at shorter wavelengths than 1Å the efficiency will generally be lower but the wall absorption will also be less. As most windows are thin this absorption effect is generally not significant when compared to the changes that occur in detection efficiency as the wavelength is altered.

The uses of thermal neutrons span many topics.[7 - 12] By observing both or either the energy and momentum exchanges that occur upon scattering information is gained concerning the distribution and dynamics of both nuclei and unpaired electronic spins in condensed matter. In this report the current topics under study are grouped into three categories.

a. Structural Studies[7,10,11]

Which includes both magnetic and glass structures as well as the conventional studies of nuclear distribution.

b. Inelastic Studies[8,9,10,12]

Concerning such topics as magnon and phonon dispersions and molecular motion in liquids.

c. Diffuse Scattering Studies[9,10,13,14]

As well as the study of point defect agglomerates this also includes the study of non-stoichiometry, alloy phases, and magnetic moment distribution determination.

A more detailed description of these subjects is given in Appendix I. Samples used for these studies are either single crystals, where scattering is discreet or randomly orientated materials, such as powders, polycrystals, liquids, glasses etc. where the scattering is averaged over all orientations. The scattering measured from a single crystal specimen, whether it be elastic coherent, inelastic or diffusive will always require a specification of an azimuthal angle. The specimen orientation will have to be rigorously defined in relation to the incident and scattered beams, Fig. 3. A randomly orientated scatterer will have the scattering distributed evenly around the incident beam subject to certain geometric considerations concerning the incident beam divergence and specimen shape. Thus for orientated scattering centre studies any extended detector system must provide information on both the scattering angle 2θ and azimuthal angle. For randomly orientated scatterers the scattering angle 2θ only is of consequence and detectors set around each scattering cone may be series coupled. Thus in general a PSD system for single crystal studies will be two-dimensional whereas for random scattering centre studies it will be one-dimensional.

The studies outlined in this section may be performed on existing neutron scattering instruments. The characteristics of these instruments are used as a guide for PSD requirements in relationship to counting rate and resolution. Table I in conjunction with Appendix I shows typical parameters of these instruments. From Table I it can be seen that the positional resolutions around the scattering arc are grouped about two extremes. The high momentum ($\underline{K}$) resolution such as for powder diffraction requires arc

TABLE I TYPICAL INSTRUMENTAL PARAMETERS

Instrument	Incident Energy Range meV	Range of scattering vector Å $^{-1}$	Present Maximum Arc (2θ) resolution mm/metre	Present Flight path resolution %
Powder diffractometer	12 - 106	0.2 - 12.0	1.5	Not applicable
Single crystal diffractometer	12 - 150	0.2 - 16.0	2.0	Not applicable
Inelastic time-of-flight	1 - 32	0.5 - 8.0	40	1.0
Inelastic crystal spectrometer	8 - 100	0.5 - 8.0	5	Not applicable
Diffuse time-of-flight	1 - 5	0.04 - 2.0	50	3.0
Diffuse monochromatic	1 - 5	0.04 - 2.0	50	Not applicable
Small angle scattering	1 - 5	0.005 - 0.3	2.5	Not applicable
Total cross-section	0.2 - 5	0.6 - 2.5	< 2.0	Not applicable

resolution of 0.15 to 0.2 cms/metre flight path. Whereas for lower K resolution this figure lies between 3.0 and 5.0 cms/metre flight path. At this point it must be stressed that certain experiments performed on high resolution instruments do not necessarily need such high resolution. For instance powder diffractometers are frequently used for amorphous studies where such high K resolution is not required. In certain other cases the use of large samples will be the limiting factor in angular resolution which will mean that the figures given in Table I are an over-estimate. The flight path uncertainty for a time-of-flight instrument must, in general, be better than 1%. Thus the thickness of the neutron detection medium for such machines must be less than 1.0 cms/metre flight path. These results may be summarised as follows in Table II.

TABLE II GENERAL PSD SPECIFICATIONS

REQUIREMENT	LOW K RESOLUTION	HIGH K RESOLUTION	COMMENT
Co-ordinates	1 and 2	1 and 2	
Positional Resolution	1.5 - 10.0 cms	0.1 - 0.5 cms	Sample - Counter distance 0.5 - 2.0 metres
Thickness Time-of-Flight	< 1.0 cms	< 1.0 cms	
Thickness Continuous Beam	No restriction	No restriction	

3 NEUTRON DETECTION

3.1 Reactions

Primary ionisation by neutrons is a negligible effect and detection of thermal neutrons can only be made indirectly by using a few induced nuclear reactions. These reactions give rise to energetic charged particles which may subsequently be detected by gas ionisation, scintillation effects or electron hole production in semi-conductors. A neutron detector must therefore consist of a neutron converter and a charged particle detector. In some cases it is possible to find a material which combines both properties. In other cases two materials are used either in physically separate states or in an intimate mix. Reactions that are commonly employed for thermal neutron detection are:

(i) $^{10}B + {}^{1}n \rightarrow {}^{7}Li^{*} + {}^{4}He \rightarrow 0.48$ MeV γ ray + $^{7}Li + {}^{4}He + 2.3$ MeV (93%)

$^{7}Li + {}^{4}He + 2.79$ MeV (7%)

(ii) $^{3}He + {}^{1}n \rightarrow {}^{3}H + {}^{1}p + 0.77$ MeV

(iii) $^{6}Li + {}^{1}n \rightarrow {}^{3}H + {}^{4}He + 4.79$ MeV

(iv) Gd + $^{1}n \rightarrow Gd^{*} \rightarrow \gamma$ ray spectrum $\rightarrow$ conversion electron spectrum (up to 170 KeV)

(v) $^{235}U + {}^{1}n \rightarrow$ fission fragments + ~ 80 MeV

(vi) $^{239}Pu + {}^{1}n \rightarrow$ fission fragments + ~ 80 MeV

The cross-sections and individual particle energies for these reactions are shown in Table III.

All the reactions other than (iv) have reaction cross-sections that are inversely proportional to neutron velocity for low energies. The departure from a $\frac{1}{v}$ dependence is very marked in the case of Gadolinium. Total cross-sections for (i) - (iv) are shown in Figure 4. Because of the sharp fall in cross-section at higher energies Gadolinium is relatively less sensitive to high energy background neutrons than is a $\frac{1}{v}$ neutron converter. However the conversion electrons produced by the gamma spectrum from the Gadolinium have rather small energies, $\lesssim$ 200 KeV.

TABLE III CAPTURE REACTION PARAMETERS

REACTION	Cross-Section for 1 Å Barns	PARTICLE ENERGIES MeV		
$^{10}B(n,\alpha)^{7}Li$	2100	α 1.47	^{7}Li	0.83 (93%)
$^{3}He(n,p)^{3}H$	3000	p 0.57	^{3}H	0.20
$^{6}Li(n,\alpha)^{3}H$	520	α 2.05	^{3}H	2.74
$^{nat}Gd(n,\gamma)$	17000	Conversion electrons: 0.07 → 0.172		
$^{157}Gd(n,\gamma)$	74000	"	"	"
^{235}U fission	320	~ 80		
^{239}Pu fission	410	~ 80		

Ignoring the effect of any non-ionising absorption (e.g. detector wall absorption) the efficiency of detection of neutrons can be expressed by the equation

$$\varepsilon = \xi (1 - e^{-N\sigma_a t})$$

where the efficiency ε is given in terms of the capture of $(1 - e^{-N\sigma_a t})$ neutrons. N is the number of converter nuclei, σ_a is the absorption cross-section for the process and is generally energy dependent and t is the thickness of the detector. Of the neutrons captured a fraction ξ results in an output pulse from the detector. This may arise from poor detector geometry, other competing capturing processes for the charged particles or from a low efficiency for the neutron/charged particle conversion.

3.2 Gas Detection

For gas ionisation detectors the value of ξ is near unity. The gas counters in present operation use reactions (i) and (ii) for thermal

neutron detection with gases of BF_3 (enriched in ^{10}B) and ^3He. In both cases the gas fulfills the function of converter and detector. The operating pressures vary between 0.5 and 10.0 atmospheres for the capture gas. The efficiencies of $^{10}BF_3$ and ^3He are shown in Fig. 5. Both ^{10}B and ^3He have capture cross-sections that vary linearly with wavelength within the thermal region. The percentage efficiencies are thus shown as a function of χ which is given by

$$\chi = \text{gas pressure (atm)} \times \text{thickness (cm)} \times \text{wavelength } (\text{Å})$$

No account has been taken of the detector geometry. Appendix III shows that an ideal detector has an efficiency of either 100% or 50 - 90% according to the signal/background ratio. A 70% efficiency would require a value of 16 atm cm Å for ^3He and 23 atm cm Å for $^{10}BF_3$. Typical detector diameters are in the range 1.0 - 5.0 cm which means a resulting pressure for 1 Å neutron detection of 16.0 - 3.0 atmospheres for ^3He and 23.0 - 4.6 atmospheres respectively for $^{10}BF_3$. Thus to obtain an optimum efficiency with a gas detector less than 5.0 cms thick a high pressure device is required.

3.3 Foil Detection

In this method the converter is in the form of a foil which is placed in close contact with a charged particle detector. The geometry of the foil must be such that the charged particles created by neutron capture or fission can escape from the foil into the adjacent detector. With the exception of (ii) all the reactions mentioned can be used for this method.

The use of ^{10}B foil is first considered. Neutron capture in ^{10}B results in a 1.47 MeV α particle and a 0.83 MeV ^7Li ion. The detection is made by measurement of the α particle emitted in the reaction. In pure ^{10}B this has an average range of 3.8×10^{-4} cm and is emitted isotropically. If the geometry in Fig. 6 is used (i.e. the α particles are detected on the remote side from neutron incidence) then for a foil thickness greater than the α range (3.8×10^{-4} cm) only the last part of the foil will emit α particles that can be detected in the charged particle detector.

For an α particle range r the efficiency ε of such a detector for a foil thickness t is given below. Σ is the neutron absorption coefficient in cm^{-1} and is equal to

$$\Sigma = N\sigma_a$$

where N is the number of atoms cm^{-3} and σ_a is the absorption cross-section at the wavelength of incidence for the (n,α) reaction

$$\varepsilon = \tfrac{1}{2}(1 - e^{-\Sigma t})\left(1 + \frac{1}{\Sigma r}\right) - \frac{t}{2r} \qquad t \leqslant r$$

$$\varepsilon = \tfrac{1}{2}\, e^{-\Sigma t}(e^{\Sigma r} - \Sigma r - 1)/\Sigma r \qquad t \geqslant r$$

The efficiency of a ^{10}B foil as a function of thickness is shown in Fig. 7 for $\lambda = 1\text{Å}$. The maximum efficiency of such a detector is very low. However, this geometry is the worst possible. The maximum efficiency for a (n,α) foil occurs when the thickness is equal to the α range. When t = r for ^{10}B 10.5% of 1 Å neutrons are absorbed. This represents the maximum possible efficiency with a single ^{10}B foil.

The efficiency of a ^{6}Li foil is even lower. The optimum thickness (t = r) in this case is 10.9×10^{-4} cm with an associated efficiency of ~1% for the Fig. 6 geometry. The maximum efficiency i.e. the total percentage of neutrons stopped by this thickness of foil is 3% at 1Å.

The low fission cross-sections for reactions (v) and (vi) give lower efficiencies. Detectors using these reactions are often used as beam monitors as their efficiency is lower and they only remove a small fraction of the beam.

The foil with the highest cross-section is Gadolinium. The nuclear reaction in this instance is a capture γ reaction. The low energy γ spectrum[15] results in a large number of conversion electrons. The ratio of captured neutrons to conversion electrons is just less than unity.[16]

Using the geometry of Fig.6 the efficiency of the detector foil is given by

$$\varepsilon = \tfrac{1}{2}\, s\, \Sigma\, e^{-\alpha t}\,(1 - e^{-(\Sigma - \alpha)t})/(\Sigma - \alpha)$$

where $\Sigma = N\sigma_a$, t is the foil thickness and s is the number of conversion electrons formed for each capture neutron. α is the extra screening coefficient averaged over 2π steradians and over orientation for an infinite foil. Following Rauch et al[16] a value of

$\alpha = 2.07 \times 10^3 \text{ cm}^{-1}$ is used.

For natural Gadolinium the efficiency is shown in Fig. 7 and is a factor of just greater than three better than ^{10}B. If ^{157}Gd is used with a cross-section of 74,000 barns at 1 Å the resulting efficiency is much increased (Fig. 7).

The detection of neutrons by foils must be made with multiple foils if a high efficiency is to be obtained. By the careful positioning of foils and charged particle detectors it is possible to achieve high efficiencies. Rauch et al[16,17] have shown that for ^{157}Gd foil an efficiency of over 70% may be obtained with a particular converter/foil geometry.

3.4 Scintillation Detection

Scintillation detectors have been widely used for thermal neutron detection. These have generally been made by mixing the neutron converter intimately with the phosphor. Such systems are $^{6}Li(ZnS)$ and $^{10}B(ZnS)$, where the recoiling particles give rise to scintillations in the ZnS. The difficulty in obtaining a high efficiency lies in the self absorption of light in the scintillation medium. Experimentally the maximum efficiencies obtained for these mixes within the thermal region are less than 50%: This restriction might be avoided by the use of some of the more standard transparent scintillators in a Gadolinium foil sandwich. All scintillation detectors have the disadvantage of being fairly sensitive to γ radiation.

3.5 Background

A high thermal neutron detection efficiency is not the only criterion for an ideal detector. The detector must also be insensitive to the background radiation which is usually experienced in thermal neutron studies. The main sources of background are fast neutrons and γ rays.

To be insensitive to fast neutrons the neutron converter must have a low cross-section for the higher energy neutrons. This is realised

in the case of absorption cross-sections that have a 1/v dependence. The fast neutron response is even further reduced in the case of Gd where the cross-section falls more rapidly with increasing energy. Fig. 8 shows that in cases where the measured fast neutron background is insignificant the ideal detector is 100% efficient whereas for a significant background the ideal efficiency lies between 50% and 90%. (See Appendix III.)

γ-ray intensities around thermal neutron scattering instruments on a reactor face are typically of the order of 10^2 - 10^4 photons $s^{-1}cm^{-2}$. The effect of this background can be reduced by shielding the detector, but the amount of material required is considerable e.g. tens of centimetres of lead around the whole detector. It is preferable to minimise the recorded counts from γ-rays by careful detector design and electronic discrimination. For a gas counter operating in the ionisation or proportional mode the amount of ionisation produced is dependent on the total energy dissipated in the detector. In a well designed detector the whole of the energy of the charged particles resulting from the (n,α) and (n,p) reactions is dissipated within the sensitive region, (i.e. detector dimensions > range of charged particles). In general for gases the energy lost by electrons from γ-capture is small compared with the energy dissipated from the proton or α particle and separation between the neutron and γ-ray pulses can be made by pulse height analysis. The difficulty of neutron-γ separation is accentuated in the case of a solid detector due to the higher densities involved. Any solid detector must therefore be kept thin to reduce γ-capture and energy dissipation from resulting electrons. Wraight et al[18] have demonstrated that some discrimination against γ-radiation can be obtained by pulse shape analysis, although this can result in the loss of true neutron counts. The γ-radiation problem, although considerable in present reactor environments, can be of negligible proportions if detectors are mounted on guide tubes or very long flight tubes.

3.6 Positional Resolution

The ultimate positional resolution of a PSD is proportional to the charged particle range in the neutron converter. For solid converters in the form of foils or an intimate scintillator/converter mixture

this range is typically of the order of 10^{-4} - 10^{-3} cms. As this figure is much lower than the present positional resolution required solid converters have no inherent resolution limitation.

In the case of gas detectors the charged particle range is a real restriction on the positional resolution and is in fact the limiting factor in the resolution obtained with gas devices. When neutrons interact with ^{3}He or $^{10}BF_3$ the two resulting charged particles are emitted isotropically and collinearly from the compound nucleus. The positional resolution is not identically equal to the total range of the charged particles but is given by the centre of gravity of the total ionisation produced i.e. the ionisation centroid. This centroid describes a sphere around the position of neutron capture and the positional resolution will be equal to the projection of this sphere onto the electrode plane. Figure 9 shows a plot of the ionisation as a function of distance for one atmosphere of $^{10}BF_3$, calculated using the cross-sections of Whaling[19]. The position of the centroid is also shown. Thus for one atmosphere of $^{10}BF_3$ the ultimate positional resolution is $\pm$ 0.28 cm.

The dependence of centroid on pressure for ^{3}He and $^{10}BF_3$ is shown in Fig. 10. The use of pure ^{3}He gives poor positional resolution and to reduce the centroid range a stopping gas has to be employed. The stopping gas is generally a heavy gas which does not detract from the ionisation effect of the ^{3}He. A common stopping gas to use in this instance is Krypton. The addition of a second gas will reduce the Helium content for a given total gas pressure and hence will reduce the detection efficiency. This effect is shown in Fig. 11, where the efficiency is plotted against centroid radius for different total pressures. The corresponding points for $^{10}BF_3$ are also shown for comparison. As may be seen a 1 atm. total pressure detector of ^{3}He has both poor efficiency and positional resolution at 1 Å for a 10 cm length of gas. $^{10}BF_3$ on the other hand has approximately the same efficiency as the maximum for ^{3}He but has a much lower centroid radius.

The addition of a stopping gas such as Kr to a ^{3}He detector whilst reducing the centroid radius also increases the sensitivity to γ-radiation. The maximum energy that the γ induced electrons can dissipate by travelling over the longest possible path length in the

detector must be substantially lower than the energy dissipated by the charged particles created in the $^{3}He\ (n,p)^{3}H$ process. Kjems[2] has shown that for a 50 cms long cylindrical detector the maximum stopping gas pressure of Kr that may be added to 2 atm ^{3}He is 0.8 atm. This limitation can only be calculated for a given counter geometry and must be considered when using Fig. 11.

P S D SYSTEMS FOR THERMAL NEUTRON SCATTERING

To date position sensitive detection systems have been developed using gas counters, scintillation arrays, barrier counters and other devices. Most of these have been associated with charged particles but a few have been extended to enable the positional detection of thermal neutrons. In this section we shall review PSD systems with special regard to the detection of thermal neutrons. All PSD's fall into one of two groups; either digital or analogue devices. The former consist of individual elements which give a quantised position of the detected particle. The analogue devices rely on the ratioing of a measured quantity such as charge, and require a degree of normalisation to give the particle position.

4.1 Gas Counters (General)

Gas counters consist essentially of a single wire anode with a coaxial cylindrical cathode (Fig. 12) and fall into four classes dictated by the main characteristics of the voltage/current curve (Fig. 12). Below the Geiger region (V) detectors are usually operated along either the ionisation plateau or in the proportional region. In each of these modes the output pulses, measured with a suitable output time constant and impedance, are proportional to the energy dissipated in the initial ionisation. In the ionisation mode the initial ions alone give rise to the pulse which is generally small for gas reactions involving neutron capture. In the proportional mode the primary electrons are accelerated to such an energy that avalanches are produced which multiply the original ionisation. Because of the dependence on the initial ionising energy both modes are favourable for thermal neutron work as they enable a good discrimination against γ-radiation to be made (Section 3.5). Simple gas counters utilising reactions (i) and (ii) section 3.1 are in common use in thermal neutron scattering experiments. The gas fillings are BF_3 (enriched in ^{10}B) and ^{3}He at pressures of 1 - 10 atmospheres. Due to the lower energy of the ionisation products in ^{3}He (0.76 MeV)

this gas can only be used in the proportional mode. ^3He is chemically less reactive than BF_3 but costs proportionately more. The choice of gas filling will depend on individual requirements.

4.2 Ionisation and Proportional Detectors

Position sensitive neutron detectors have been made operating in both the ionisation and proportional modes.

Allemand and Jacobe[4,5] have pioneered the use of multiple electrode BF_3 ionisation chambers and both one and two-dimensional detectors are being built for use at the Institut Max Von Laue-Paul Langevin, Grenoble. The principle is indicated in Fig. 13. In their latest devices, the electrodes are made from copper vacuum deposited on glass and the electrode geometry can easily be varied to give cartesian or polar coordinates matched to the requirements of the experiment. The efficiency of a prototype one-dimensional detector was quoted as 10% at 1.2 Å with a positional resolution of 5.2 mm (private communication). The development version has an increased thickness of gas along the neutron direction which should result in efficiencies of approx. 50%. The two-dimensional detector is expected to have an overall efficiency of approx. 20% at 1.2 Å and a positional resolution of 10 mm. The logic circuitry sets an upper count limit of $2 - 5 \times 10^4$ counts/second.

Analogue linear proportional PSD's are used at present on the MARC-type inelastic spectrometers (Kjems[2]). The linear (one-dimensional) detector consists of a normal cylindrical ^3He or BF_3 counter with the anode wire replaced by a resistive wire with a readout from each end. For wire resistances in the region of 40 to 2000 Ω/cm positional information is obtained by the charge ratio. For higher resistance wires, > 400 kΩ/cm, the position is obtained by delay line techniques; measuring the time dependence of the signal to each end.[20,21] The best positional resolution for a resistive wire neutron detector has been obtained with central anode wires of quartz coated with aquadag. Resolutions of 8 mm for 2 atm ^3He + 0.8 atm Kr have been reported by Kjems[2] using wires of resistance 2.5 kΩ/cm.

A prototype multiwire resistive proportional counter is being constructed by Harwell Counter Group for use at the PLUTO and DIDO reactors. The device uses the charge sharing technique and will have 30 wires with a sensitive area of 60 x 15 cm^2. This work arises from a proposal of Egelstaff and Forsyth.[22]

Multiwire proportional counters are used widely in high energy physics experiments for measuring the positions of charged particles. The development of these counters is due to Charpak at CERN.[23] The coordinates of the detected particles are usually measured separately by two planes of counters with the wire anodes orientated at right-angles or at some other stereo angle. Such trajectory sampling techniques are impossible with neutrons where both coordinates have to be measured in the same detector. The most common method of reading out data from Charpak chambers is to treat each wire as a separate channel with its own preamplifier, delay and gating circuit. The pulses are stored in registers before being processed. Considerable efforts are being made to produce a cheap integrated circuit element to reduce the cost and size of the electronics required for each wire.

An alternative approach due to Perez-Mendez[24] avoids the use of read-out from individual wires by using a delay line technique (Fig. 14). A delay line lies at right angles across the plane of anode wires and the position of the struck wire is calculated by timing the arrival of pulses at each end of the delay line. This system clearly has advantages over the one wire per channel technique but with large area detectors there is likely to be a problem of pile-up of pulses in the delay line.

We have been unable to find any reference in the literature to the use of Charpak chambers for the detection of neutrons. In principle there seems no reason why this should not be done with gases of BF_3 of ^3He. Both position coordinates would have to be read from a single gas volume either by using the induced pulse from a cathode grid or by sharing the electrons between two crossed anode grids. It should also be possible to use converter foils of say Gd inside conventional Charpak chambers.

4.3 Geiger-Muller Counters

Gas detectors are not used in the Geiger region for thermal neutron scattering due to their sensitivity to γ-rays. The signal is much larger due to the complete ionisation of the gas but is independent of the energy of the ionising radiation making discrimination against γ-radiation impossible. The complete breakdown of the gas results in a longer recovery time than for ionisation and proportional operation which results in a lower maximum count rate. De Lima and Pullman[25] have however developed a position sensitive Geiger Counter for use with charged particles.

4.4 Spark Chambers

The spark chamber is a development of the older detector known as a spark counter. The spark counter in its simplest form consists of a pair of parallel plates (typical separation 1 cm) in a gas atmosphere with a high potential between them. The counter is used in the same way as a G M counter and suffers from the same disadvantages. When a pulsed high potential is used with this counter it becomes a spark chamber; an important device used extensively in high energy physics. The gas fillings usually involve helium, neon or argon and the principle is indicated in Fig. 15. A high voltage pulse (typically 10 - 20 kV cm^{-1}) is applied when the scintillation counters indicate that a charged particle has transversed the chamber. The pulse causes a preferential breakdown along the trail of ions left behind by the charged particle and the resulting spark lies close to the trajectory of the particle. The spark can be photographed from two or more positions and the coordinates of the particle in any gap calculated.

Many other methods of recording the spark position have been developed with the aim of making spark chambers into on-line devices. The most important of these are sonic, magnetostrictive, core and capacitive readout systems which have all been used to give on-line data usually in conjunction with computers.[26,27,28,29] The maximum counting rate is determined by different considerations in the various types of readout but in general is less than 10^3 counts/sec over the whole detector.

Spark chambers could be used as position sensitive neutron detectors provided that BF_3 or ^3He are compatible with spark chamber operations. ^4He has been widely used in spark chambers so ^3He should be a suitable filling. Alternatively a converter screen such as Gd can be used inside a conventional chamber. A prototype spark chamber containing a boron converter has been built and tested on the HERALD reactor (private communication). For neutron work the high voltage trigger pulse (obtained from the scintillation counters when using charged particles) would in general have to be derived internally from the spark chamber. For some experiments e.g. time-of-flight, this trigger pulse could be derived from other places such as a chopper, (Appendix I). For charged particles spatial resolutions of much better than 1 mm have been obtained with spark chambers. The sphere of uncertainty associated with the range of the decay products involved in neutron detection is likely to prevent this being achieved with neutrons.

4.5 Hybrid Chamber

The hybrid chamber proposed by Fischer and Shibata[29] combines multiwire proportional counters with conventional spark chambers, Fig. 16. This device was developed to avoid the expensive cost per wire of electronics for proportional multiwire counters. The hybrid chamber consists essentially of a proportional wire chamber gap which is read out by a narrow gap pulsed spark chamber and a magnetostrictive line. The electron drift space between the proportional gap and pulsed spark gap is required in high energy physics experiments to compensate for delays in associated counters and logic circuits. The electrons from a charged particle in the proportional region drift to the high field region around the anode wires and form avalanches. Some of these electrons drift through the delay region towards the spark chamber gap. If this gap is pulsed while the avalanche electrons are in it, a spark is formed which is read out in two dimensions by conventional magnetostrictive means. The high voltage pulse and its duration are controlled so that sparks form only from electron clouds and not from the few electrons that might occur in the spark gap from a background particle. The recovery time after a spark is shorter than in conventional spark chambers due to the narrower gap which allows more rapid clearing of the ions left

by the spark. Fischer and Shibata claim that the hybrid chamber is about ten times faster than ordinary spark chambers. This implies that counting rates of approximately 10^4 sec^{-1} should be possible.

As in conventional spark chambers ^3He would be a good filling gas in hybrid chambers used for neutron detection. The triggering pulse to switch the high voltage onto the spark chamber gap could be derived from the proportional plane.

4.6 Scintillation Systems

Charged radiation excitation of certain molecular and atomic systems which subsequently decay with the emission of light pulses, provide valuable methods of radiation detection. For neutrons the neutron/charged particle converter may be mixed intimately with the phosphor or be mounted as a separate screen before it. The light pulses are usually detected by means of a photomultiplier tube.

Both solid and liquid scintillators are available. For charged particles crossed strips of scintillators are commonly used to give particle positions using coincidence techniques between X and Y planes, (Fig. 17). The resolution is determined by the scintillator widths and the number of channels which can be afforded. Two-dimensional neutron position sensitive detectors must obtain both coordinates from the same plane of scintillator. A similar problem exists when measuring the position of low energy particles. An analogue technique used extensively in hospital physics[30] involves viewing a single piece of scintillator with an array of photomultiplier tubes. These are coupled to the scintillator either by fibre optics or by an optical coupling compound. The position of each scintillation is calculated from the relative sizes of photomultiplier signals.

A neutron detector using this method has been built at AWRE Aldermaston using a ^6Li (ZnS) scintillator screen.[31] The charged particles resulting from the ^6Li cause the ZnS to scintillate.

The scintillator is coupled to 23 x 5 cm diameter photomultipliers. Each scintillation is viewed by several phototubes and a mixing technique involving the signals from nearby phototubes enables a positional resolution better than the diameter of one phototube to be achieved, (0.6 cms). No development work concerning the thickness of the optical coupling, phototube separation or scintillator thickness has been done. It may therefore be possible to improve the resolution figure of 0.6 cms.

Measurements of the positions of very fast neutrons along a strip of scintillator have been made by timing the light from the scintillation to photomultipliers at either end of the strip.[32] The scintillator used had no neutron/charged particle converter deliberately added and relied on a fraction of the high-energy neutrons producing knock-on protons from the hydrogenous component. This timing method is not usable for slow neutrons as present converter/scintillator mixtures are opaque over distances of more than a few millimetres.

Scintillator arrays to give one-dimensional information for slow neutrons are in common use.[33] A possibility that might be developed is the use of annular rings of liquid scintillator for studies involving randomly orientated samples, (Fig. 18). If a solid transparent converter/scintillator mixture becomes available, it would be relatively easy to make such a device.

The scintillator technique could become very important for PSD work when coupled with a new device known as a channel plate[34,35,36]. This extension of the older channel multiplier consists of a section (approx. $\frac{1}{4}$" thick) cut from a bundle of fine glass tubes typically 40 μm in diameter. The glass is loaded with an oxide and chemically treated to produce a very thin layer of metal on the surface of the tubes. With the appropriate electric field across the plate (Fig. 19) electrons from a nearby photo-cathode can be drawn through the plate creating further electrons by secondary emission from the internal surfaces of the tubes. Due to the short length of the plate the secondary electrons preserve the original spatial information contained in the light falling on the photo-cathode. If sufficient

amplification is available and if the collector plate is made position sensitive, the spatial information can be read out.

Several possibilities exist for the collector plate. A group at the Mullard Space Science Laboratory at Dorking, Surrey are developing a resistive plane which has four point probes and employs a pulse timing technique between pairs of probes to give the position of charged particles falling on the plane.[37] Preliminary tests indicate that the position over areas of 30 - 50 cm^2 can be read off to better than $\pm$ 1 mm. A less accurate, but still acceptable collector for neutron detectors, could be made from etched copper clad circuit board with individual collectors of say $\frac{1}{2} \times \frac{1}{2}$ cm^2 or more simply still by using point electrodes on a matrix of known pitch.

For neutron work the channel plate could be used with a photo-cathode to view either a loaded scintillator or a converter foil/scintillator. The photo-cathode may be eliminated by using a Gd foil directly in front of the channel plate. Under the influence of an electric field the Gd conversion electrons would pass into the plate and produce secondary electrons directly.

Channel plates have already been used for X-ray detection with areas of approx. 1 cm^2. [38,39,40] Larger areas are required for neutron scattering experiments but plates of 5" diameter have already been produced. These devices have a high development potential for a neutron PSD but they may be costly.

4.7 Semiconductor Devices

Surface barrier detectors have been used for thermal neutron detection with the aid of a Gd foil converter.[16] Neutron detection is made by the measurement of conversion electrons produced by prompt neutron capture γ-rays in Gd. The surface barrier detectors are used for the detection of the conversion electrons. A detection efficiency of up to 70% (at a 2 Å) is claimed and each detector can be made very small. The positional information is obtained by covering an area with a large number of such detectors. A particular detector being considered would have a total area of 10 x 40 cms with elements 1 x 1 cm^2. Although the foil is thin (0.03 cm) the gamma sensitivity is fairly high. Easy discrimination is therefore not possible, although it is much better than with scintillators. The cost of covering a large

area with this type of digital PSD would be very high and in many cases would offer no advantage over a gas detector, as the positional resolutions are comparable.

Commercially made semiconductor devices are available which give the linear position of a charged particle entering the detector.[41] These devices are silicon surface barrier detectors and the position detection is made by using a resistive layer on the back of the depleted region of the detector. A signal is derived from each end of the detector which acts as a simple voltage or charge divider to give the position of the particle. In principle neutron position sensitive devices could be made by using these detectors behind a converter foil but the maximum detector areas available are currently 10 x 50 mm^2 at a cost of approx. £500 each. Their high cost makes this method unattractive.

In general, the small detection areas available with current semiconductor devices limit the use of such devices for neutron position sensitive detectors. The possibility of developing larger detection areas, cheaper detectors, or some method of loading the semiconductor directly with neutron converter, will be discussed with workers in the semiconductor field.

4.8 Bubble Chambers

Bubble chambers are three-dimensional detectors that are used for showing the tracks of charged particles in high energy physics experiments. The collection of ions resulting from the passage of an ionising particle through the detector can act as nucleating centres for boiling in a super-heated liquid. The usual liquid is hydrogen which also acts as a target material in many experiments. The magnified train of bubbles along the tracks are photographed stereoscopically and the geometry of the track reconstructed from measurements made on the film. These detectors are very bulky and data handling via film and measuring machines is very cumbersome.

The use of liquid hydrogen would not be acceptable for thermal neutron detection, although ^{3}He would seem to be a suitable filling in this respect. The complexity of such devices and the associated cryogenic systems would prohibit their general use around reactors even if some method of automatically measuring and reading out the track positions could be developed.

4.9 Qualitative Position Sensitive Devices

So far in this section only devices which would give quantitative information have been considered. Several systems which give a visual scattering pattern have been devised. These usually involve the use of a scintillator sheet viewed directly (or indirectly through an image intensifier tube) by a vidicon camera with the information being displayed on a television monitor screen. Such devices have an obvious use in the early stages of an investigation when a cursory look at the scattering patterns is desirable. It may be possible to develop means of obtaining quantitative information from such devices as methods for digitising the output from vidicon cameras viewing optical spark chambers have been developed.[42] The problem of viewing sparks is clearly easier than that of viewing single scintillations and it seems unlikely that this method could be developed to provide absolute counting rates for neutrons.

4.10 Summary of PSD Systems

The characteristics of the devices discussed in this section are summarised in Table IV.

TABLE IV - SUMMARY OF CHARACTERISTICS OF KNOWN AND POTENTIAL NEUTRON POSITION SENSITIVE DETECTORS: A - GASEOUS

Type	Filling	Dimensions (cm)	ε_o at 1Å	Resolution (cm)	Max. Rate (pulses/sec)	Co-ordinates	Digital or Analogue	No. of Elements	State
Ionisation Chamber									
1	1 Atmos.BF_3	1.5 gap x 210 length (on 150 radius) x 6 high.	8%	0.52	~2×10^4	x	D	400	Working detector - Allemand (4,*). Resolution determined by electrode geometry.
2	1 Atmos.BF_3	11 depth x 210 length (on 150 radius) x 2.5 high.	45%	"	"	x	D	"	Under construction - Allemand (4,*). Resolution determined by electrode geometry.
3	1.2 Atmos. BF_3	Double 1.5 gap x 64 x 64	20%	1.0, 1.0	5×10^4	x,y	D	64 x 64→ 4096	"
4	"	Double 1.5 gap x 64 diameter	"	1.0, ~10^o	"	r,θ	D	32 x 36→ 1152	"
Proportional Chamber									
1	2 Atmos.He^3 + 0.8 atmos. Kr.	5 diameter x 50 long	55%	0.9 (average)	~10^4	x	A	Single resistive wire	Working detector - Kjems (2) (similar detector - Abend(1))
2	10 Atmos. He^3 + 1 atmos. Kr.	2.5 diameter x 50 long	80%	≤ 1.0	~10^4	x	A	Single resistive wire	Prototype under test - AERE Counter Group (*)
3	1 atmos. BF_3	2.5 gap x 60 high x 15 length	15%	≤1.0,0.5	~10^4 - 10^5	x,y	A	30 resistive wires	Under construction - AERE Counter Group(*)
4(a)	1 atmos. He^3 (or BF_3)	Say 1.5 gap x 100x100	~10%	4.0 (0.3 if $^{10}BF_3$ used)	~10^5 direct read-out, ~10^4 indirect read-out	x,y	D,A	few x 10^4	)Possible development)(with delay line)read-out, if gas is)pressurized
(b)	5 atmos. He^3	"	~40%	0.5	"	"	D,A	"	

TABLE IV continued

Type	Filling	Dimensions (cm)	ε at 1Å	Resolution (cm)	Max. Rate (pulses/sec)	Co-ord-inates	Digital or Analogue	No. of Elements	State
Spark Chamber									
1	Boron Foil in conven-tional chamber	1.0 gap x 16.5 x 16.5	5%	0.3	$\sim 10^3$	x,y	D,A	64 x 64 4096	Prototype magneto-strictive and Ferrite core readout, Rodgers AWRE (*)
2	1 Atmos. He^3	Say 1.5 x 100 x 100	~10%	4.0	$\sim 10^3$	x,y	A	few x 10^4	Possible development (with magnetostric-tive read-out but low resolution, efficiency and counting rate)
Hybrid Chamber	1 Atmos. He^3	Say 1.0 x 100 x 100	~6%	4.0	$\sim 10^4$	x,y	A	few x 10^4	Possible development (with magnetostrictive read-out but low reso-lution and efficiency)

* Private communication.

TABLE IV - SUMMARY OF CHARACTERISTICS OF KNOWN AND POTENTIAL NEUTRON POSITION SENSTITIVE DETECTORS: B - SOLID STATE

Type	Components	Dimensions (cm)	ε at 1 Å	Resolution (cm)	Max. Rate (pulses/sec)	Co-ordinates	Digital or Analogue	No. of Elements	State
Scintillators									
1	Scint. + Photomultiplier	23 diameter	~50%	0.6	$\sim 10^3$	x,y	A	1(+ 23 phototubes)	Working detector - Holland and Pain(31) (rate limit is in the data handling system)
2	Foil + Scint. + Photomultiplier	Either annular rings up to 100 diameter or elements of few square cms.	~20%	Would depend on dimensions but typically >1.0	$\sim 10^6$	θ,x, xy	D	Few for θ, x many for x,y	Possible development, γ background may be a problem.
3	Foil + channel plate	Areas in units of 5" diam. possible at present.	~20%	0.1 - 0.2	not known	x,y	D,A	1 per channel plate	) Possible developments
4	Foil and Scint.+ channel plate	"	~20%	"	"	x,y	D,A	"	)
Semi-conductors									
1	Foil + surface barrier detector	10 x 40	~40%	1.0	$\sim 10^6$	x,y	D	400	Proposed detector - looks promising for medium resolution and small areas.

5 DISCUSSION

5.1 General

The detectors oulined in Table IV fall into the two broad classes; digital and analogue discussed in Section 4. The former class has the obvious disadvantage that for large sensitive areas and high resolutions a large number of elements would be required. It does however have a considerable advantage over the latter class in that any instability or drift in the associated electronics cannot distort the positional information over the whole detection area. This is not true of analogue devices which ratio or compute the positions from other information, and in general rely on balanced circuits. This is a potential weakness of such devices; any detector destined for regular use on a neutron scattering device should have long term stability and be relatively simple to use and maintain. The efficiencies of discrete channels can be quickly checked by scattering neutrons from a standard sample and individually correcting faulty channels. To check that a ratioing device as a whole is not distorting the scattered neutron pattern over part or all of its sensitive area is more difficult and any corrective action would, in general, require a time consuming and tedious operation to rebalance the circuits.

5.2 Detectors

(a) Gaseous Detectors

Only two gases are useful as detector media, ^{3}He and BF_3. Figures 10 and 11 show that ^{3}He cannot be used for high resolution devices unless pressures of the order of 5 atmospheres can be tolerated. This situation can be improved by the addition of a heavier stopping gas such as krypton, but even then pressures of around 2 - 3 atmospheres would be required to achieve resolutions comparable with those obtainable with 1 atmosphere of BF_3. This is an unfortunate result as BF_3 while less expensive than ^{3}He is a corrosive and hazardous gas to handle. Figure 5 shows that both gases must either present approximately 10 cms of path length to the scattered neutrons at 1 atmosphere or be pressurized in order to obtain reasonable efficiencies at 1 Å.

Pressures up to 10 atmospheres are easily accommodated in the simple cylindrical shapes used with single wire proportional counters. When multiwire neutron detectors with areas of say 1 square metre are considered, the design of the containing vessel presents problems, especially if tailored to the experimental geometry. A pressurised neutron detector would clearly be bulky and unless diaphragms were inserted and buffer zones of an inert gas used, the total volume of detector gas required would be significantly greater than that required for the multiwire structure alone. With ^{3}He costing approx. £100/litre this factor is clearly important. High pressure gaseous devices require higher EHT voltages for operation, with the attendant problems of breakdown and background noise. The operating voltages of ^{3}He are lower than for BF_3 due to the lower ionisation potential of the former and high pressure proportional counters usually employ ^{3}He for this reason.

The types of gaseous detectors available are ionisation, proportional, spark, and hybrid chambers. For two-dimensional information the efficiency is unacceptably small at one atmosphere unless a longer neutron path length is formed by stacking planes of detectors. Figures 10 and 11 show that for a one atmosphere gaseous device resolutions of $< \pm 5$ mm can only be obtained with BF_3. Electro-negative ions are known to produce problems in spark chamber operation and consequently BF_3 can be expected to prove difficult to use in this mode. None of the gaseous devices seem to offer any possibility for a one atmosphere, two-dimensional, high resolution, large area detector with reasonable efficiency.

In general, Geiger counters and spark chambers are unacceptable due to their inherently low maximum counting rate. If pressurized devices are tolerable, ionisation and proportional techniques, particularly Charpak chambers, could be used to give good resolution and reasonable efficiencies for two-dimensional detectors.

For one-dimensional information the problem of efficiency is reduced as the detector can in general be made thick with respect to the beam direction. Allemand et al have used this technique very effectively with their one-dimensional multi-ionisation chamber array (Fig. 13). Proportional detectors could also be used. Again BF_3 is the only choice at one atmosphere if positional resolutions of $< \pm 5$ mm are required.

(b) Scintillation and Semiconductor Devices

Scintillators can either be loaded with a neutron converter or used with a converter foil, whilst semiconductors can only be used with the latter. Due to the higher densities involved and the consequent reduction of the charged particle ranges these devices do not suffer from the resolution problems inherent with unpressurised gases. Scintillators can be used with photo-multipliers or channel plates and in either case the PSD can be digital or analogue. Scintillation counters are digital when isolated photomultipliers are used to view individual scintillators (multi-counter arrays). These become analogue devices when overlap occurs between adjacent photomultiplier signals (Scinti-camera). For channel plates the geometry of the collector plate (Fig. 19) will determine whether the PSD is digital or analogue. High resolution digital devices say $< \pm 5$ mm, will be limited to small detection areas otherwise the number of channels becomes unmanageable (e.g. 4×10^4 for a metre square detector with ± 2.5 mm). Coarser resolutions necessarily imply less channels. The resolution of analogue devices is to a large extent dependent on the electronics used.

In general the efficiency of all these devices is less than 50% and is very dependent on the geometry and type of converter used. A problem that can be expected with this type of device is associated with gamma ray sensitivity, the higher densities involved give higher gamma conversion probabilities and the overall background problem is consequently greater than with gases. This effect can be reduced by keeping the detector volumes to a minimum. In this respect the semiconductor detectors (depletion layers approximately 50 μm) are clearly superior to liquid and solid scintillators where 1 mm is probably the least thickness which can be used.

Of the devices discussed in 5.2(b) only loaded scintillators have been extensively developed for thermal neutron detection detection.[33] With the exception of Rauch et al[16] and Feigl et al[17] very little work has been done on semiconductor neutron detectors. Recent developments[38,39,40] have shown that channel plates can be used for x-ray detection. We suggest that converter foils, semiconductor detectors and channel plates are all potentially useful for neutron position sensitive detectors and should be further investigated.

5.3 Instruments

The matching of individual PSD systems to particular instruments will require a more detailed study, (including consideration of cost and readout facilities), than can be given in this report. However certain of the more important features can be discussed at this stage and these are summarised in Table V. The designations A, B and C denote our assessment of relative merits. The A category is used for the combination of PSD and instrument which would be worth developing; the B category for combinations that have some potential if further development work is performed on the PSD and/or the instrument. The C category denotes unsuitability for use or development. The allocation of these categories to each type of instrument will be discussed in the following sections. Special emphasis is given to powder diffraction requirements since these pose the most exacting conditions on a PSD system with regard to the positional determination of neutron capture, see Tables I and II for reference.

(a) Powder Diffraction

Present powder diffractometers retain a high degree of resolution by the use of suitable Soller slit collimators before and after the monochromator and before the detector. These are designated α_1, α_2 and α_3 respectively, (Fig. A1 Appendix I). Soller slits cannot be effectively used in front of position sensitive detectors. The α_3 collimator in a conventional machine enables an extended sample to be used whilst retaining a high degree of resolution; the sample size

TABLE V ASSESSMENT OF RELATIVE MERITS OF PSD FOR VARIOUS TECHNIQUES

PSD	Powder Diffraction	Single Crystal Diffraction	Amorphous Materials	Inelastic Time of Flight	Inelastic Crystal Spectrometer (MARC)	Diffuse Time of Flight	Mono-chromatic Diffuse	Small Angle Scattering
Multi- Ionisation Chamber	A	A	B	C	A	B	B	A
Multi-Proportional Chamber	A	A	B	C	A	B	B	A
Resistive Wire Proportional Chamber	C	B	B	C	A	C	C	B
Spark Chamber	C	C	C	C	C	C	C	C
Hybrid Chamber	C	C	C	C	C	B	C	C
Scintillators								
a) Scinti-camera	B	B	B	C	B	C	C	B
b) Channel Plate	B	A	C	C	B	C	C	A
Semi-Conductor (with converter foil).	B	A	B	C_p, B_s	B	C	C	A
Simple Multi Counter Array	C	C	A	A	C	A	A	C

s ≡ single crystal studies; p ≡ random scatterers.

in this instance does not contribute to the resolution. However with the removal of the α_3 collimator the "after sample" resolution is heavily dependent on sample size. The effective angular divergence is given by: (Sample radius + counter uncertainty)/f where f is the flight path from sample to detector. We consider a gas detector, as the inherent counter uncertainty is greatest with this system. For $^{10}BF_3$ at one atmosphere the counter uncertainty is approx. 0.3 cms. Thus for a flight path of one metre the effective collimation before the detector is 0.45^{o}, 0.7^{o} and 1.3^{o} for 1, 2 and 4 cm diameter samples respectively. Typically, α_3 collimators have divergence angles of 0.1^{o} to 0.5^{o}. This limits a PSD detector to operation with $\leq$ 2 cm diameter samples for an equivalent resolution.

The signal to background for a PSD detector is likely to be higher for sample independent background and equal to a conventional device for sample dependent background. By counting over all the angular range simultaneously the gain over a single counter instrument is in the region of 200 whilst the loss due to sample volume will be between 4 and 16. This assumes that sufficient sample is available to enable a conventional machine to utilise a full 4 cm diameter sample, thus gains in the time between 10 and 50 may be experienced compared to a single detector instrument.

Of the PSD systems considered, those best suited to powder diffraction measurements are the ionisation and proportional chambers. Due to the high resolution required the measurement of the scattering cones is usually performed in the equatorial plane (Fig. 3). Resolutions of the order of 0.3 - 0.5 cms are required which are possible by using multi-electrode gas detectors filled with one atmosphere BF_3 and spanning a total scattering angle of 100^{o}. To obtain an efficiency > 40% the detector would have to be of the order of > 10 cms thick. However as no movement of the detector is needed this does not pose a structural problem. To span such an arc (1 metre radius) and match the required resolution using scintillators

or semiconductor detectors would be prohibitively expensive. The low count rate that can be realised with spark and hybrid chambers eliminates them for such measurements.

A simple multi-counter which consists of a series of annular counters each at different scattering angles and each following a Debye cone (Figs. 3, 18) would give an enhanced count rate at each position but the density to which such a system can be grouped is likely to be too low to provide the high resolution needed for powder diffraction. If there is sufficient demand for a fast general powder diffractometer with medium resolution then in our opinion such an instrument should incorporate a PSD. A gas detector system operating in either the ionisation or proportional mode is the most suitable PSD provided the gas filling is such that the centroid radius lies between 0.3 - 0.5 cms. The multi-ionisation chamber developed by Allemand et al[4] is now commercially available[43] in a form compatible with powder diffractometry.

(b) Single Crystal Diffraction

Large samples are not generally used for single crystal studies as apart from the low availability of large single crystals the extinction in these is too high. The diffraction from a single crystal is also much less divergent than from powder specimens. These points result in a PSD system for single crystal studies being of greater value in most instances than for powder studies. Egelstaff and Forsyth[22] have shown that for single crystal studies a gain of 30 may confidently be realised with a large PSD device. Further gains may be realised if the materials under study contain larger unit cells. A good example of the potential of PSD for single crystal diffraction can be seen in the development of an automatic x-ray diffractometer capable of measuring 12,000 reflections per hour from large chain molecules.[44] Position sensitive detectors for neutron single crystal diffraction may be considered in one of two ways. A large stationary detector covering the major part of the scattering plane and capable of

azimuthal angle measurement has the advantage of covering a very large number of reflections simultaneously. Physically such an instrument is not easy to design and the number of read out channels for such a device will be very large if angular resolutions of $< 1^{o}$ (= 1.8 cm/metre) are to be obtained. The alternative detector consists of a smaller PSD mounted on the conventional counter arm. This could be moved to measure different reflections in the conventional manner. For many biological specimens measured with incident wavelengths of 0.9 - 2.0 Å, resolution limits the measurements to $< 50^{o}$ (2θ); hence a smaller PSD would be preferable. The small prototype two-dimensional PSD (Section 4.2d) at present under design at AERE Harwell will be installed on a single crystal diffractometer and should give valuable information concerning the use of PSD systems in general for thermal neutron scattering.

We cannot envisage the use of spark or hybrid chambers in this instance as their low counting efficiencies and their pulsed requirements make them less attractive than other methods. Further development is needed if a small detector light enough to be mounted on a counter arm and with good efficiency is to be produced. Gas detection is sufficiently advanced to be immediately applicable whereas semiconductor and scintillators with channel plate detectors appear to have considerable potential in this field, but require further development.

(c) Amorphous Materials Scattering

The structure study of amorphous materials requires a different resolution from either of the cases so far discussed. To perform these studies instruments are needed which are capable of going to large scattering vectors, but the overall angular resolution required is not high when compared to powder diffraction measurements. For amorphous systems the scattering is isotropic around each scattering cone. Maximum intensity may be realised if at each scattering position, i.e. each measured 2θ value, the maximum possible azimuthal arc is covered. As the resolution required is not so high as for the powder diffraction case single detectors may be placed at

individual counter positions and be made such that the array follows the scattering cone. To perform these measurements we favour a single multi-counter array as being most likely to produce the highest gains in measured intensity. A smaller gain may be made by replacing a single stepped detector on an existing instrument by a position sensitive system mounted in the equatorial plane.

It is worth noting that the present Harwell LINAC total scattering spectrometer, used for amorphous studies, has a very short sample to detector distance which would allow the major part of the scattering sphere to be covered with a reasonable size PSD. However this would no longer be possible if a current suggestion to extend this distance to several metres is adopted.

(d) Inelastic Time-of-Flight Scattering

Much of the previous discussion concerning amorphous materials is equally applicable to the study of molecular dynamics and other inelastic studies not involving single crystals. These studies also do not in general require a high momentum resolution. Thus the scattering as a function of 2θ may be investigated by detectors well spread in angle which can have quite a coarse positional resolution around the 2θ arc. As the scattering is isotropic around the scattering cone the highest count rate gain is obtained by single detector positions which follow the scattering cone but which require no positional information around the azimuthal arc, (simple multi-counter array).

For single crystal studies typical counter separations of 3^{o} with an angular resolution of 0.8^{o} are adequate for the majority of current measurements. In our opinion the current practice of using individual element detectors provides the best system. For flight paths of greater than a metre elliptical high pressure ^{3}He proportional detectors (as on the 7H1R twin chopper spectrometer, Harwell) are to be

recommended as their efficiency and background discrimination characteristics are better than for present scintillation detectors.

Development of converter foil detectors which are inherently thinner would enable shorter flight paths to be used while preserving the present flight path resolution of $< \pm 1\%$. This resolution may be easily achieved for 50 cm flight paths by utilising Gadolinium foil converters backed by semiconductor devices or channel plates.

(e) Inelastic Crystal Spectrometry

We consider that the standard triple axis instrument has no requirement for a PSD. On such a machine energy analysis is performed by rotating the analyser crystal and detector in a 1:2 ratio (θ - 2θ scan).[8] The replacement of the existing counter assembly with a PSD would remove the need for rotating the detector about the analyser crystal axis. The analyser crystal would still have to be rotated to measure the energy spectrum and the required information would appear at a discrete position in the PSD. Consequently only a small part of this detector would be used at each analyser setting. The advantage of saving one mechanical axis would be outweighed by the disadvantages of having to provide larger shielding, a higher count rate due to integrating the background over the whole PSD and possibly calibration problems if the efficiency varied across the detector.

Kjems and Reynolds[2,45] have extended the normal triple axis machine to enable the simultaneous collection of neutrons within a range of scattering angles from the analyser. This Multi Angle Reflecting Crystal Spectrometer (MARC) consists of a large analysing crystal very near the sample and a linear resistive wire PSD. Although at the present time only resistive wire PSD's have been used we consider that comparable resolutions and efficiencies may be obtained using multi-ionisation chambers which have the distinct advantage of being digital devices.

Crystal spectrometers using filter techniques for analysis utilise the largest area of scattered beam as possible. As no momentum resolution is imposed on the detector angle, a single detector with as large an acceptance angle as possible is needed.

(f) Diffuse Time-of-Flight Scattering

Both single and powder (or polycrystalline) samples are measured on this type of instrument. For samples that have randomly orientated scattering centres the highest gain in measured intensity may be made using a simple multi-counter array with individual detectors that span the azimuthal arc. This is illustrated in Figure 18 for a scintillation detector.

The scattering from single crystal specimens has in general an azimuthal angle dependence. Information out of the equatorial plane is only of value if a large proportion of the scattering arc is covered. As the resolutions involved are coarse and the areas large, approx. 1.5 m^2, this requirement is best met by a two-dimensional multi counter array of pressurised gas detectors. This comment is also relevant for random scatterers if signals from detectors around each azimuthal arc are coupled.

(g) Monochromatic Diffuse Scattering

The use of a non pulsed monochromatic beam of neutrons for diffuse studies removes the constraints on detector thickness. However as with the time-of-flight system the highest gain to be achieved with randomly orientated scatterers is by covering as large a proportion of the azimuthal arc as possible. Single proportional detectors may be used or with the further development of liquid scintillators a series of curved annuli would be suitable (Fig. 18).

For single crystal measurements a multi-counter array is most suitable. Since the detector thickness is not a restriction cheaper low pressure gas counters can be used end on to the scattered beam.

(h) Small Angle Scattering

As the total range measured is small, typically less than 10^{o} (2θ), the size of a PSD for such measurements can be quite small even though sample to detector distances are very large (typically > 2 metres). With a 40 cm square detector with 2-dimensional positional resolution of $\pm$ 1 cm a scattering vector range of up to 0.3 $\mathring{A}^{-1}$ can be measured with a 2 metre flight path and wavelengths between 4 and 10 $\mathring{A}$. Any development of a small angle scattering apparatus should include the investigation of PSD systems as these look to be particularly useful in this field.

Most of the two-dimensional PSD's that have been considered are applicable to these studies, especially the multi-ionisation and proportional chambers.

Scintillator devices although susceptible to high background may be exploited if SAS instruments are mounted on guide tubes where the low γ-background enables the scintillation technique to be used with advantage.

5.4 Conclusions

The fields most immediately amenable to PSD systems are single crystal diffraction, powder diffraction and small angle scattering experiments. Amorphous studies and time-of-flight measurements with both short and long wavelength neutrons are, in general, better served by multi-counter arrays. The variation of the triple-axis spectrometer known as the MARC inherently requires a PSD. The conventional triple axis spectrometer, filter spectrometer, and polarized neutron diffractometers are best used with single detectors.

With our preference towards digital devices we consider the following to be the most promising of the PSD's considered:-

(a) Multi-electrode ionisation and proportional chambers (e.g. Allemand et al[4]) for both one and two-dimensional detectors.

(b) Converter foil/scintillators or converter foils directly with semiconductors or channel plate detectors.

There is clearly no PSD which can be universally used in thermal neutron scattering. The multi-electrode ionisation and proportional chambers come nearest to meeting this criterion. One-dimensional detectors of this type (Fig. 13) are very suitable for powder diffraction and MARC spectrometry and could be made to approximate to multi-counter arrays by varying the effective resolution. We can envisage a PSD connected to a small computer where the individual input channels may be soft-ware grouped to give variable resolutions and hence count rates for the angular divisions required. Two-dimensional multi-electrode chambers are suitable for single crystal diffraction and small angle scattering experiments but have the disadvantage of low efficiencies.

Since Allemand et al are well advanced with the development of multi-electrode chambers we suggest that the type of PSD outlined in (b) above should be developed. If this can be done successfully, one and two dimensional high resolution digital devices, thin but with reasonable efficiencies, will become available without the complication of pressurised gaseous fillings.

ACKNOWLEDGEMENTS

We are grateful for helpful discussions with colleagues in the Neutron Beam Research Unit, Rutherford Laboratory, members of the Materials Physics and Electronics/Applied Physics Divisions at AERE, Harwell, and of various University neutron scattering groups, Dr A L Rodgers of A W R E, Aldermaston, Mr R Allemand of CEN Grenoble, Dr J Kjems of the Research Establishment, Risö, Mr P W Sanford and other members of the X-ray Astronomy Group at the Mullard Space Science Laboratory, Dorking.

APPENDIX I

THERMAL NEUTRON STUDIES

In section 2 we divided the studies performed with thermal neutrons into three main categories. This appendix indicates the requirements made by these studies in connection with the development of PSD and multi-counter arrays. A general outline of the fields of study is also given together with details of the instruments involved in the measurements.

A1.1 Structural Studies

The neutron spectrum emanating from a research reactor has a peak typically at a wavelength of 1 Å. These wavelengths are of the order of crystal spacings with the result that such neutrons undergo diffraction obeying the Bragg criterion $2d \sin\theta = \lambda$. The placing of a single crystal of sufficient dimensions and at the correct orientation in the 'white' reactor beam enables a monochromatic beam of neutrons to be selected.

The scattering of a monochromatic beam by a single crystal specimen yields discrete maxima in three dimensions. The separation of the maxima is inversely proportional to the lattice spacing. Thus for very large unit cell materials, such as those of biological interest, a great number of reflections simultaneously satisfy the Bragg condition.

The scattering of monochromatic neutrons by a powder or a polycrystalline material again gives rise to maxima - Debye rings - but in this case the orientational dependence of the sample has been lost and the scattering is symmetric about the central beam. Thus only the scattering angle (2θ) has to be defined. Although pure diffraction is absent in a glass or a liquid the scattering maxima, corresponding to the distances of closest approach in the radial distribution function, follow Debye like rings having symmetry about the incident beam direction.

So far the discussion has only concerned the scattering of neutrons by the nucleus which for an isolated scattering centre is isotropic. However, the neutron possesses a magnetic moment of 1.9 nuclear magnetons which results in interactions with atomic magnetic moments.[7,10] The scattering by a single magnetic ion is angularly dependent and has a form factor fall-off. Neutron diffraction may thus be used for the study of magnetic structure as well as nuclear and very large advances have been made using this technique.

Instruments have been developed for the structural study of single crystals, powders, liquids and glasses. The instruments used for powder studies use relatively large samples and so require collimation before and after the sample. These Soller slit collimators enable extended samples to be used without a high loss in angular resolution. To improve the angular resolution the counters of powder diffractometers are typically placed at up to 100 cms from the sample centre. With these dimensions resolutions of 0.2^{o} (2θ) can be achieved. Machines that are used for the study of amorphous materials are very similar to those in use for powder studies except that a higher scattered intensity is obtained by relaxing the resolution, which is no longer required for this type of work.

Single crystal machines on the other hand do not require the use of Soller slits and long sample-detector distances as the diffraction peaks are very narrow. Thus a typical monochromatic single crystal diffractometer will have a sample-detector distance of less than 50 cms. "White beam" methods (Laue) can be used with neutrons. However in the UK this technique has only been used for specimen orientation alignment using scintillator detection coupled with a photographic film, but proposals for the ILL, Grenoble include modified Laue techniques using both photographic and counter detection.

Diagrams of both powder and monochromatic single crystal diffractometers are shown in Fig. A1. It will be noted that the single crystal instrument has a goniometer mounted on it to enable three degrees of freedom for the specimen which are needed to place any reflection within the detector.

A1.2 Inelastic Scattering

The energies of thermal neutrons (1.0 - 200 meV) are of the same order as those of lattice vibrations and many molecular modes of oscillation and vibration. For the study of lattice vibrations the momentum changes associated with the inelastic interactions are also within the range measurable with the neutron technique. By conducting high resolution coherent scattering experiments the dispersion relations associated with phonon and magnon modes and their interactions may be studied. Molecular systems and diffusive motions of light atoms may be investigated by incoherent inelastic scattering. These measurements do not in general require such a stringent resolution with respect to the momentum transfers and hence scattering angles do not need to be so well defined.

Single crystal inelastic studies, like those of elastic phenomena, are discretely distributed in three dimensions requiring the accurate alignment of the specimen with respect to the incident and scattered beams. Randomly orientated specimens on the other hand such as powders, polycrystals, liquids and glasses have the azimuthal angle dependence averaged over all orientations; with the result that the scattering pattern is of a form analogous to the Debye cones for elastic powder diffraction. Only the single scattering angle 2θ has then to be defined.

The experimental requirements for inelastic scattering are twofold. Both energy and momentum are conserved on scattering. This requires both the incident and scattered energies and momenta to be specified in order to gain the maximum information concerning the scattering centre. The momentum requirement is, of course, eased in the case of molecular and diffusive systems.

Many instruments have been developed to investigate inelastic scattering. These have included devices relying on pulsed beams to measure the energy exchange. Pulsing is produced by a pulsed source or by a beam pulsing device, (a chopper). Unpulsed techniques have also been used relying on crystal diffraction for energy analysis. Filter methods can be used to measure the scattered energy and to produce incident energies within a given range. However the two main categories of time-of-flight (a) and crystal spectrometers (b) represent most of the requirements that will be made on the detection system.

(a) A diagram of a 'twin chopper' time-of-flight machine is shown in Fig. A2. A white neutron beam is incident on the first chopper which then pulses the beam. Because of the relative phasing of the second chopper to the first only a narrow velocity band of neutrons may pass the second chopper. Thus an essentially mono-energetic beam of neutrons is incident on the specimen. Interaction with phonons etc., within the specimen result in neutrons being scattered with different energies at different angles. The energy separation relies on the fact that the different energy neutrons will take a different time to traverse a distance of several metres to the detectors. The scattered flux is collected at up to 30 angles and into an array of up to 1000 time channels defining the velocities of neutrons leaving the sample. In order to obtain a sufficient spread in the velocity components of the scattered beam a flight path of typically 100 - 300 cms must be used.

Repeated pulsing of the incident beam builds up a time-of-flight or energy spectrum at each detector position.

Incident energies for time-of-flight investigations range from 1.5 to 150 meV. At these energies flight path resolutions of 1% are adequate which means that at a typical flight path of 1.5 metres detectors with an effective thickness along the beam direction of 1.5 cms may be used. The momentum resolution resulting from the detector area may range from approx. 1% to 10% with a detector width of 5.0 cms at a 1.5 metre flight path.

(b) This apparatus uses crystal reflections to monochromate and analyse the incident and scattered beams respectively. As in a normal diffractometer a reactor 'white' beam is incident on a monochromating crystal (Fig. A2) which is set to reflect a particular wavelength of neutrons. This monoenergetic beam is incident on the sample where it undergoes energy and momentum exchange. The scattered beam is then energy analysed by detecting the scattered beam through a second crystal - the analyser. The incident and scattered momenta are defined by the beam directions before and after the sample.

Kjems and Reynolds[2,45] have developed the triple axis machine to extend the data collection rate. By replacing the conventional analyser crystal and its collimator by a large analysing crystal set very near the sample, the scattering from several angles may be measured simultaneously. The detection over the angular range covered by the extended analyser is performed by a linear position sensitive detector, Fig. A2.

By using crystal techniques for monochromating and analysing, both the energy and momentum resolution are greatly improved over mechanical systems.

Both techniques outlined above are used to advantage for the study of inelastic phenomena. The study of phonons and magnons in single crystals gives rise to discrete maxima in scattered neutron intensity which are usually well separated in space. When using the time-of-flight instrument for these measurements the phonon or magnon peaks measured at any one time, will not necessarily be all from the same symmetry direction; a requirement often needed in a dispersion study. Thus a large amount of data is collected, all energy channels at all angles, but only a fraction can contain vital information. The use of a crystal spectrometer for these single crystal studies does have certain advantages. This instrument has a low background, as a well shielded detector is used away from the main beam. The instrument also looks at discrete regions of energy-momentum space and can be automated to step along any chosen direction. Thus measurements can be made at regular intervals along directions of high symmetry. The energy and, more important, the momentum resolution can be made much higher than the equivalent time-of-flight machine. However, in instances when a maximum amount of information is required at many momentum transfers and over a range of energies the time-of-flight instrument has a definite advantage.

The use of powder, polycrystalline or amorphous samples where scattering is only characterised by the single scattering angle is best suited to the time-of-flight technique. Best use can be made of the instrument in this instance by relaxing the resolution around the azimuthal angle; and at each 2θ scattering angle covering as large an amount of the scattering cone as possible.

A1.3 Diffuse Scattering

The effects of irradiation and heat treatment on condensed systems can result in the formation of defect clusters. These may range from point defect clusters produced by fast neutron irradiation[46] to small precipitates of solute atoms in a heat treated allowy.[47] Such defects will cause lattice strain which in certain cases is very extensive. Other defective systems can be caused by doping a stoichiometric material with a small percentage impurity to produce non-stoichiometric defects.[48] These again may give rise to associated lattice strain, which together with the original defect can produce pronounced diffuse scattering. Magnetic systems may also be defective. Here an originally pure magnetic material such as ferromagnetic iron or nickel may be perturbed magnetically by the introduction of a small fraction of non-magnetic ions. The original moment distribution will be perturbed, and this effect may be measured by observing the diffuse magnetic scattering.[13]

The technique may also be used to look at non-defective systems such as the study of covalency. The measurement of the magnetic scattering from a paramagnetic material yields a form factor for the magnetic ions. The shape of this form factor may be used to determine the degree of covalency in the nominally ionic material.

Diffuse scattering occurs away from the main Bragg diffraction maxima. However other competing effects such as multiple Bragg diffraction can occur in this region. A convenient method for removing these effects is to perform the experiments with neutrons of an incident wavelength greater than λ_c where

$$\lambda_c = 2\, d_{max}$$

and d_{max} is the maximum interplanar spacing of the crystal lattice. For these longer wavelengths only the (000) reflection occurs from the host lattice. Several methods for the measurement of elastic diffuse scattering have been developed based on this criterion:

(a) Differential measurements (monoenergetic beam)

(b) Differential measurements (time-of-flight)

(c) Small angle scattering.

(d) Total cross-section technique.

(a) A diagram of the typical apparatus is shown in Fig. A3. A monoenergetic beam of neutrons between 5 Å and 20 Å is selected by means of a mechanical velocity selector. The scattered neutrons are collected at a number of detector positions. The counter widths are typically 5.0 cms and the sample-detector radius is approx. 100 cms. The sample in this instance may have to be cooled to remove the inelastically up-scattered neutrons which will also be contributing to the measured intensity. An alternative method of inelastic removal is by pulsing the monoenergetic beam by a single chopper. This then enables only elastically scattered neutrons to be measured using a time-of-flight separation.

(b) A similar method to that described in (a) has been developed for the study of magnetic defect systems[50], and is shown in Fig. A3. A chopped beam is incident on the sample which is usually cooled. The elastic scattering may be measured by time-of-flight (using one time channel) at a series of angles. Wavelengths used are from 5 Å to 10 Å with a resulting scattering vector range of 0.04 $Å^{-1}$ to 1.7 $Å^{-1}$. Angular resolution is like (a), of the order of $\pm$ 1.5°.

(c) In order to study larger defect and alloy phenomena than those accessible by the former two types of instrument a technique analogous to small angle x-ray scattering has been developed.[51] This is shown in a typical form of Fig. A4. The incident wavelength can be as large as 10 Å and measurements at as low a scattering angle of 2° can be made. The angular resolution requirement of such an instrument is greater than that of (a) and (b) and is of the order of 0.2°.

Diffuse scattering may also be measured as a function of wavelength by measuring the transmission of a beam of monoenergetic neutrons, Fig. A4. A beam in the range 5 - 20 Å is incident on a specimen with a resolution of approx. 5% in wavelength. The transmission of the cooled sample is measured with a detector in the straight through beam position. Alternatively the transmission of an ambient defective sample may be compared to a non-defective standard specimen. This technique enables much smaller defect concentrations to be measured as a larger sample can be placed in the beam than with (a) and (b). Typical sample sizes are 2.5 - 10 cms in thickness in the beam direction.

APPENDIX II NEUTRON BEAM INSTRUMENTS IN THE U K A E A

Instrument	Reactor/ Source	Majority Measurement	Detector System
DELILAH	HERALD	Powder Diff. amorphous studies	Movable single, 5 cm diameter, 1 atm., BF_3 end on to beam.
VANESSA*	HERALD	Powder Diff.	Movable bank of 9, 5 cm diameter, 1 atm. BF_3 counters, end on.
FIONA	HERALD	T-O-F Diff. from powders	Fixed bank of 8, 5 cm diameter LiF/ZnS scintillators.
BADGER I BADGER II	DIDO) DIDO)	Powder Diff. and general purpose diffracto-metry	)Movable single 2.5 cm)diameter, 1 atm. BF_3 end on)to beam.
CURRAN	DIDO	Powder Diff.	Movable bank of 5, 5 cm diameter, 1 atm. BF_3 counters end on to beam.
PANDA*	PLUTO	Powder Diff.	Movable single, 5 cm diameter 1 atm. BF_3, end on to beam.
7H2R GUIDE* TUBE	PLUTO	Long wave-length diffra-ction bias towards biolo-gical materials	Movable single, 2.5 cm diameter, 1 atm. BF_3, end on to scattered beam.
LIQUIDS* SPECTROMETER	DIDO	Amorphous studies	Movable single, 5.0 cm dia-meter 2 atm., ^3He, end on.
TOTAL SCATTER-ING	HARWELL LINAC	Amorphous studies	Fixed bank of 4 groups of 2.5 cm diameter, 4 atm. ^3He, side on to beam.
MARK VI (1) MARK VI (2)	DIDO) DIDO)	Single crystal diffraction	Movable single, 2.5 cm dia-meter, 1 atm. BF_3, end on to beam.
LAUE	PLUTO	Single crystal alignment	Li/ZnS scintillator with photographic plate.
FERRANTI (1) FERRANTI (2) FERRANTI (3)	PLUTO) PLUTO) PLUTO)	Single crystal diffraction	Movable single, 2.5 cm, dia-meter, 1 atm. BF_3, end on to beam.

APPENDIX II continued

Instrument	Reactor/ Source	Majority Measurement	Detector System
POLARIZED BEAM (1) POLARIZED BEAM (2)	PLUTO))) PLUTO)	Magnetic single crystal diffraction	Movable single, 2.5 cm, diameter, 1 atm. BF_3 end on to beam.
SINGLE CHOPPER SPECTROMETER	HERALD	Molecular and quasi-elastic inelastic scattering	Fixed bank of 8 groups of 2, 2.5 cm. diameter, 4 atm. ^3He, side on to beam.
ROTATING CRYSTAL SPECTROMETER	HERALD	Inelastic scattering, coherent and quasi-elastic	Movable bank of 4 groups of 2, 4 atm. 2.5 cm. diameter, ^3He, side on to beam.
EDNA	HERALD	Inelastic quasi-elestic molecular modes	Fixed bank of 1 group of 4, 2.5 cm. diameter, 4 atm. ^3He, side on to beam.
COLD SOURCE INSTRUMENT	DIDO	Inelastic Molecular studies	Fixed bank of 13 groups of 2 atm. 2.5 cm. diameter, BF_3 side on to beam covering large proportion of arc.
		Phonon studies	Fixed bank of 24 groups of $^6Li/ZnS$ scintillators.
LONG WAVELENGTH SPECTROMETER	DIDO	Molecular studies	Fixed bank of 9 groups of 2 atm. 2.5 cm. diameter BF_3 side on to beam covering large proportion of arc.
TWIN CHOPPER	PLUTO	Inelastic coherent scattering	Fixed bank of 30 6 atm. elliptical 5 x 2.5 x 5 cm. ^3He detectors.
THREE AXIS*	DIDO	Inelastic coherent scattering	Movable single 5.0 cm diam. 2 atm. ^3He end on to beam.
THREE AXIS	PLUTO	Inelastic coherent scattering	Movable single 5.0 cm diam. 1 atm. BF_3 end on to beam.
		Used as Be filter spectrometer	Movable bank of 3 pairs 5.0 cm diameter 1 atm. BF_3 side on to beam series coupled.
DEFECT APPARATUS (cold source)	HERALD	Nuclear diffuse scattering	Fixed bank of 16,5 cm. diameter 2 atm. BF_3 side on to beam.
TRANSMISSION APPARATUS	HERALD	Nuclear diffuse scattering	Single 2.5 cm. diameter 1 atm. BF_3 along the beam.

APPENDIX II continued

Instrument	Reactor/ Source	Majority Measurement	Detector System
GLOMMETER*	PLUTO	Nuclear diffuse scattering	Fixed bank of 13 groups of 9 detectors, 2.5 cm. diameter, 1 atm. BF_3. side on to beam.
GLOPPER*	PLUTO	Nuclear and magnetic diffuse scattering	Movable bank of 5 groups of 9 detectors, 2.5 cm. diameter, 1 atm. BF_3, side on to beam.
CURRAN*	PLUTO	Small angle scattering from large centres	Movable single 2.5 cm. diameter, 1 atm. BF_3, end on.

* Indicates that the instrument is at present under review or development (May 1972).

APPENDIX III

OPTIMUM DETECTOR EFFICIENCY

The fractional error associated with the statistical measurement of (sample and background) count and background count in a normal experiment is given by

$$\left[\frac{E_s}{S}\right]^2 = \frac{1}{S^2}\left[\frac{S + B}{t_{S+B}} + \frac{B}{t_B}\right]$$

where E_s is the statistical error in measuring the sample count rate S and B is the background count rate, t_{S+B} and t_B are the times for measuring the (sample + background) count rate (generally called the sample count) and the background count rate respectively.

For a given total measuring time T

$$T = t_{S+B} + t_B$$

divided in the ratio R between the measurement on the sample and its background and the background alone.

$$R = t_{S+B}/t_B$$

the fractional error $\frac{E_s}{S}$

is given by

$$\left[\frac{E_s}{S}\right]^2 = \frac{(R + 1)}{R\,S^2T}\left[S + B\,(R + 1)\right] \qquad \ldots(1)$$

By minimising expression (1) with respect to the ratio R; the ratio of the counting times to give the least statistical error for a total counting time T is:

$$R = \left[\frac{S + B}{B}\right]^{\frac{1}{2}}$$

In this instance the fractional error is

$$\left[\frac{E_S}{S}\right]^2 = \frac{1}{S^2 T}\left[(S + B)^{\frac{1}{2}} + B^{\frac{1}{2}}\right]^2 \qquad \ldots(2)$$

For many detectors the background count rate is mainly determined by the fast neutron flux as the γ background is usually removed by electronic discrimination. In this instance

$$S = \tau\,(1 - e^{-N\sigma_t x})$$

and

$$B = \phi\,(1 - e^{-N\sigma_f x})$$

where τ and ϕ are the absolute thermal and fast neutron fluxes at the detector. σ_t and σ_f are the thermal and fast neutron capture cross-sections for the detector whilst N and x are the atomic density and detector thickness respectively. By rewriting (2) we obtain:

$$\left[\frac{E_S}{S}\right]^2 = \frac{\left[(r + 1)^{\frac{1}{2}} + 1\right]^2}{S\,T\,r}$$

$$\tau\left[\frac{E_S}{S}\right]^2 T = \frac{\left[(r + 1)^{\frac{1}{2}} + 1\right]^2}{r\,(1 - e^{-N\sigma_t x})}$$

where

$$r = \frac{(1 - e^{-N\sigma_t x})}{(1 - e^{-N\sigma_f x})} \times \frac{\tau}{\phi} = \frac{S}{B}$$

The quantity $\tau\left[\frac{E_S}{S}\right]^2 T$ is an effective error and is directly proportional to the fractional error on S. $T\tau$ represents the total number of thermal neutrons incident on the detector during the experiment and of course has no efficiency dependence.

For $\tau/\phi = 1$ and using values of $N\sigma_t$ and $N\sigma_f$ appropriate to $^{10}BF_3$ as an example we obtain S/B > 50 in the efficiency range 0% to 100%; i.e. $(1 - e^{-N\sigma t x})$ lies between 0 and 1. The curve of the effective error against efficiency is plotted in Fig. 8 for S/B > 50. The minimum error is obtained for a detector of 100% efficiency.

When $\tau/\phi = 10^{-3}$ S/B ratios for $^{10}BF_3$ lie between 0.025 and 0.2 for the whole efficiency range. The curve for S/B < 0.2 is also plotted in Fig. 8 and shows that a minimum error occurs at 71.6%. The error lies within 15% of this minimum value for 50% - 90% efficiencies. The conclusion is that for high measured signal to background ratios the ideal detector is 100% efficient for thermal neutrons whereas for low measured signal to fast neutron background ratios the detector efficiency should be between 50% and 90%. In general this means that ideally counters used for structural studies should be 100% efficient while those used for inelastic and diffuse scattering studies should be in the range 50% - 90%.

REFERENCES

1. ABEND, K, Jülich report, Jül - 582 - ZE (1969).
2. KJEMS, J, Risö report - 229, (1970).
3. ABEND, K, SCHMATZ, W, SCHELTEN, J and MULLER, K D, Nucl. Instrum.Meth. 83, (1970), 111.
4. ALLEMAND, R, BOURDEL, J, JACOBE, J, CONVERT, P, and ROUNDAUT, E, NOTE LETI/MCTE 70/2308 , Centre d'Etudes Nucléaires de Grenoble, (1970).
5. JACOBE, J, DARIER, P and CONVERT, P., NOTE LETI/70-1252 - NU, Centre d'Etudes Nucléaires de Grenoble, (1970).
6. JACOBE, J, and CONVERT, P., Institut Max von Laue-Paul Langevin, Report ST-71/240, Grenoble, (1971).
7. BACON, G E, "Neutron Diffraction", Oxford Univ. Press, 2nd Ed. (1962).
8. EGELSTAFF, P A, "Thermal Neutron Scattering", Academic Press, (1965).
9. GUREVICH, I I, and TARASOV, L V, "Low Energy Neutron Physics", Amsterdam: North Holland Pub. Co., (1968).
10. MARSHALL, W, and LOVESEY, S W, "Theory of Thermal Neutron Scattering", Oxford Univ. Press, (1971).
11. ARNDT, U W, and WILLIS, B T M, "Single Crystal Diffractometry", Cambridge Univ. Press, (1966).
12. TURCHIN, V F, "Slow Neutrons", IPST, Sivan Press, (1965).
13. LOW, G G E, "Inelastic Scattering of Neutrons", IAEA, Vienna, (1965), 413.
14. MARTIN, D G, Phil. Mag. 5, (1960), 1235.
15. GROSHEV, L V, LUTSENKO, V N, DEMIDOV, A M and PLELKHOV, V I, "Atlas of γ-ray Spectra from Radiative Capture of Thermal Neutrons", London: Pergamon Press, (1959).
16. RAUCH, H, GRASS, F, and FEIGL, B, Nucl. Instrum. Meth. 46, (1967), 153.
17. FEIGL, B, and RAUCH, H, Nucl. Instrum. Meth. 61, (1968), 349.
18. WRAIGHT, L A, HARRIS, D H C, and EGELSTAFF, P A, Nucl. Instrum. Meth. 33, (1965), 181.
19. WHALING, W, Handuch der Phys. 34, (1958), 193.
20. BORKOWSKI, C J, and KOPP, M K, Rev. Sci. Instrum. 39, (1968), 1515.
21. BORKOWSKI, C J, and KOPP, M K, IEEE Trans. Nucl. Sci., NS-17, (1970), 340.
22. EGELSTAFF,P A, and FORSYTH, J B, Neutron Beam Advisory Panel Report (1969), 13.
23. CHARPAK, G, BOUCLIER, R, BRESSANI, T, FAVIER, J, and ZUPANCIC, C., Nucl. Instrum. Meth. 62, (1968), 262.
24. GROVE, R, KO, I, LESKOVAR, B, and PEREZ-MENDEZ, V., UCRL-20255, (1971).

25. DE LIMA, J J P, and PULLAN, B R, Nucl. Instrum. Meth. 96, (1971), 77.
26. LILLETHUN, E, MAGLIC, B, MANNING, G, STAHLBRANDT, C A, TAYLOR, A E., and WALKER, T G, Nuvo Cim. (Suppl.) 2, (1964), 310.
27. PEREZ-MENDEZ, V, and PFAB, J M, Nucl. Instrum. Meth. 33, (1965), 14.
28. BOUNIN, J, MILLER, R, NEUMANN, M, SARMA, J, and SHERRARD, H, IEEE Trans. Nucl. Sci. NS-11, (1964), 321.
29. FISHER, J, and SHIBATA, S, Int. Conf. Instrum. for High Energy Physics, Sept. 1970 Dubna, USSR (BNL 14899).
30. MOODY, N F, PAUL, W, and JOY, M L G, Proc. I E E E 58, (1970), 217.
31. HOLLAND, B G, and PAIN, L F, N P Memo/113, SNA, AWRE (1971).
32. NEILSON, G C, GLAVINA, C, DAWSON, W K, IYENGAR, K V K, and MACDONALD, W J, Nucl. Instrum. Meth. 81, (1970), 301.
33. HARRIS, D H C, et al "Inelastic Scattering of Neutrons", IAEA Vienna, (1963), 107 and 171.
34. GUEST, A J, HOLMSHAW, R T, and MANLEY, B W, Advanc. Electron. 28A, (1969), 471.
35. GUEST, A J, Mullard Technical Paper TP 1248, 1971.
36. GUEST, A J, and POOKE, R, Proc. Conf. Electro-Optics, (Brighton 1971), 277.
37. SANFORD, P W, and STUMPEL, J, Private Communication.
38. PARKES, W, GOTT, R, and POUNDS, K A, Trans. IEEE Nucl. Sci. NS-17, (1970), 360.
39. GOTT, R, PARKES, W, and POUNDS, K A, Trans. IEEE Nucl. Sci. NS-17, (1970), 367.
40. GOTT, R, PARKES, W, and POUNDS, K A, Nucl. Instrum. Meth. 81, (1970), 152.
41. Nuclear Diodes Inc., Prairie View, Ill. USA.
42. CRAWFORD, J F, DOBINSON, R W, OSMON, P E, and STRONG, J A, Nucl. Instrum. Meth. 52, (1967), 213.
43. Le Materiél Téléphonique, Quai Alphonse Le Gallo, Boulogne, France.
44. XUONG, N, and VERNON, W, Amer. Crys. Assoc. Symposia, 1972, (Proceedings), p.55.
45. KJEMS, J K, and REYNOLDS, P A, "Neutron Inelastic Scattering", IAEA, Grenoble, 1972.
46. CLARK, C D, MITCHELL, E W J, and STEWART, R J, "Crystal Lattice Defects", 2, (1971), 105.
47. RAYNAL, J M, SCHELTEN, J, and SCHMATZ, W, J. Appl. Cryst. 4, (1971), 511. CLARK, C D, and MEARDON, B H, Nature Physical Sciences, 235, (1972), 18.
48. CHEETHAM, A K, FENDER, B E F, and STEEL, D., Solid State Commun. 8, (1970), 171.
49. QUERCIGH, E, Nucl. Instrum. Meth. 41, (1966), 355.
50. LOW, G G E, Advanc. Phys. 18, (1969), 371.
51. SPRINGER, T, and SCHMATZ, W, Bull. Soc. fr. Minér. Crist. 90, (1967), 428.
52. RAUCH, H, Proceedings of IAEA Conference on Instrumentation for Neutron Inelastic Scattering Research, Vienna, Dec. 1969, page 275.

FIGURES

Figure No.

A1 Schematic diagrams of:

(a) Powder diffractometer.

(b) Single crystal diffractometer.

A2 Schematic diagrams of:

(a) Time-of-flight (inelastic) instrument.

(b) Three axis instruments.

(i) standard

(ii) MARC

A3 Schematic diagrams of:

(a) Monoenergetic diffuse scattering apparatus.

(b) Time-of-flight diffuse scattering apparatus.

A4 Schematic diagrams of:

(a) Transmission apparatus (diffuse scattering).

(b) Small angle scattering apparatus.

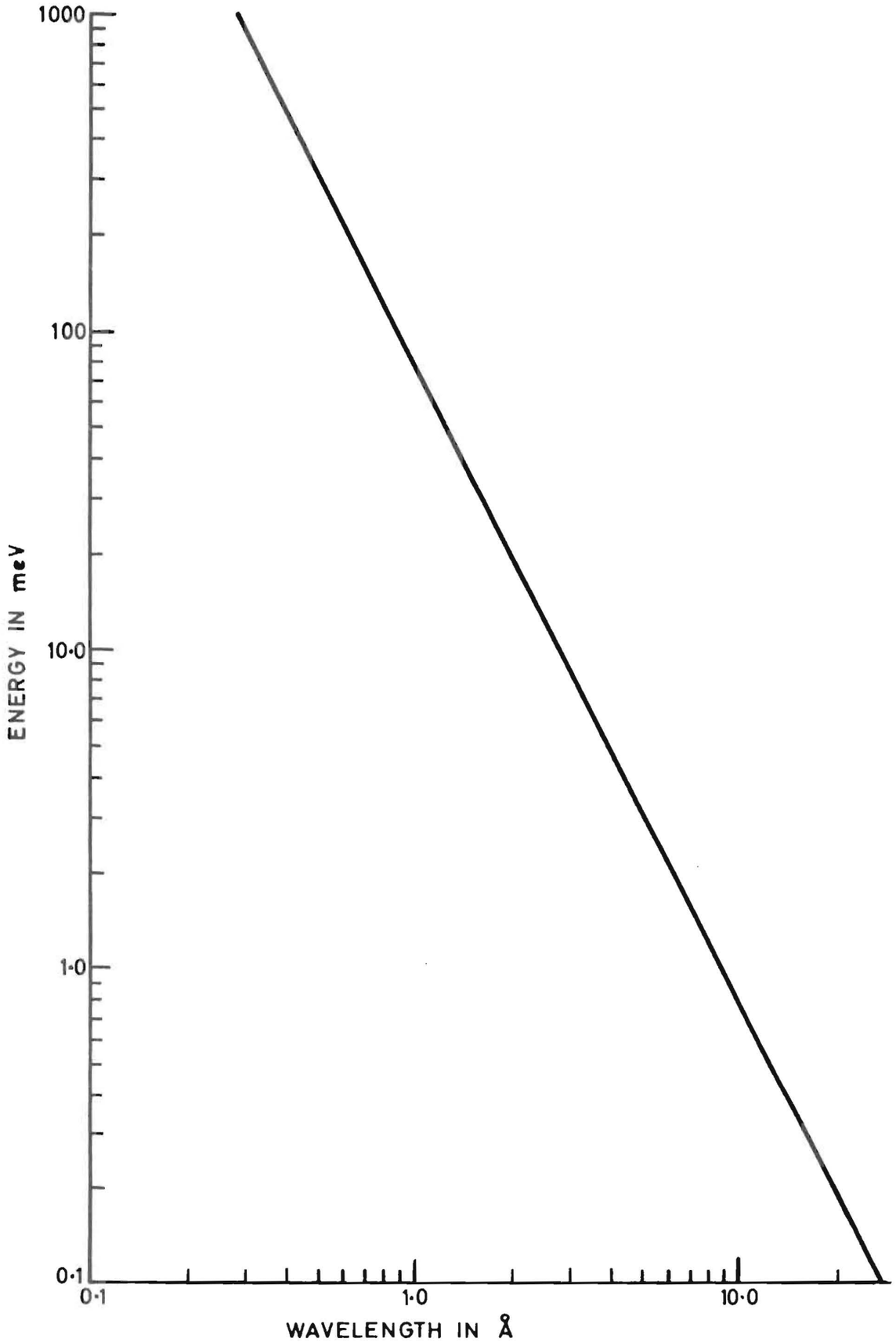

Fig. 1. NEUTRON ENERGY-WAVELENGTH RELATIONSHIP

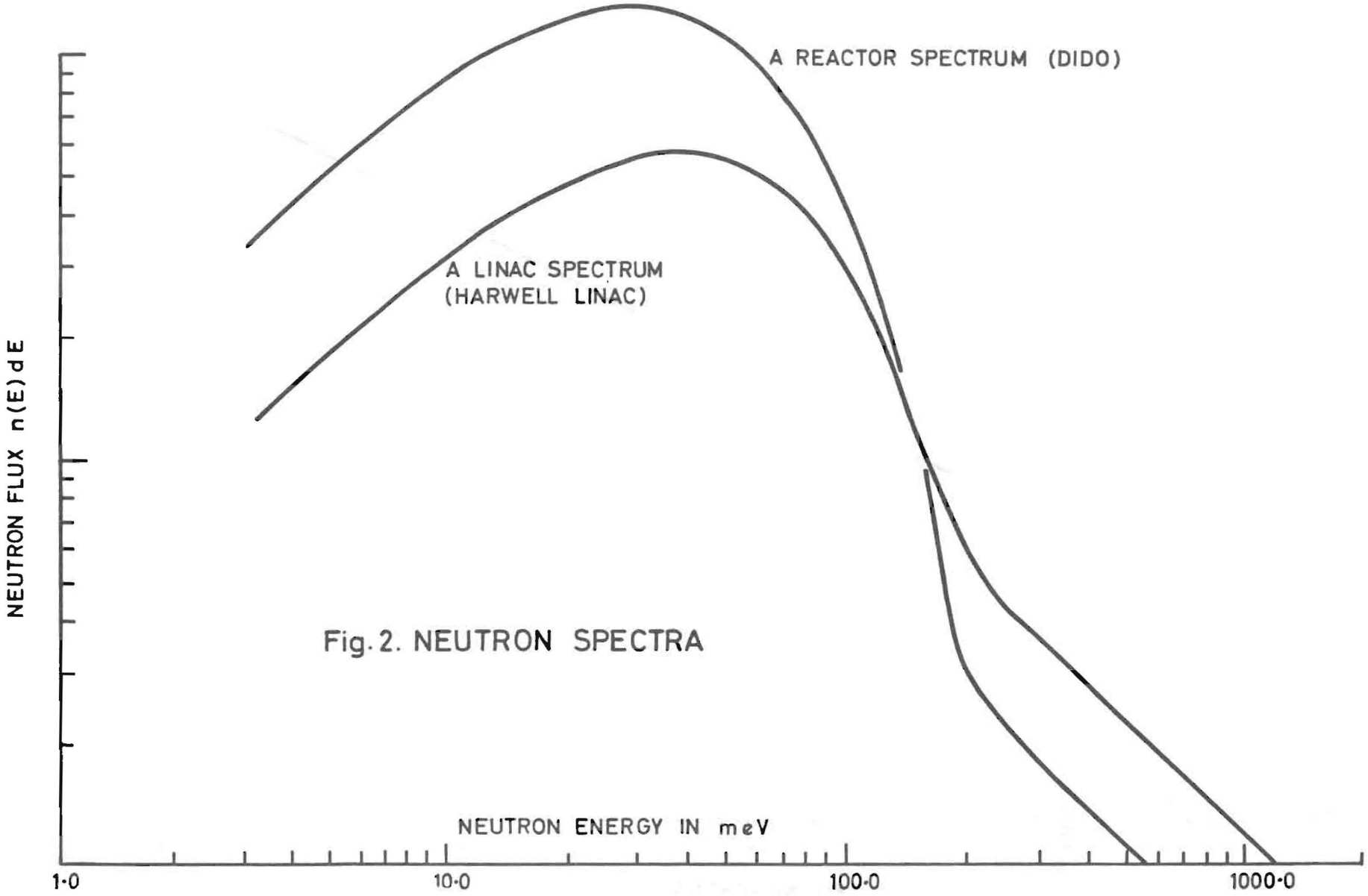

Fig. 2. NEUTRON SPECTRA

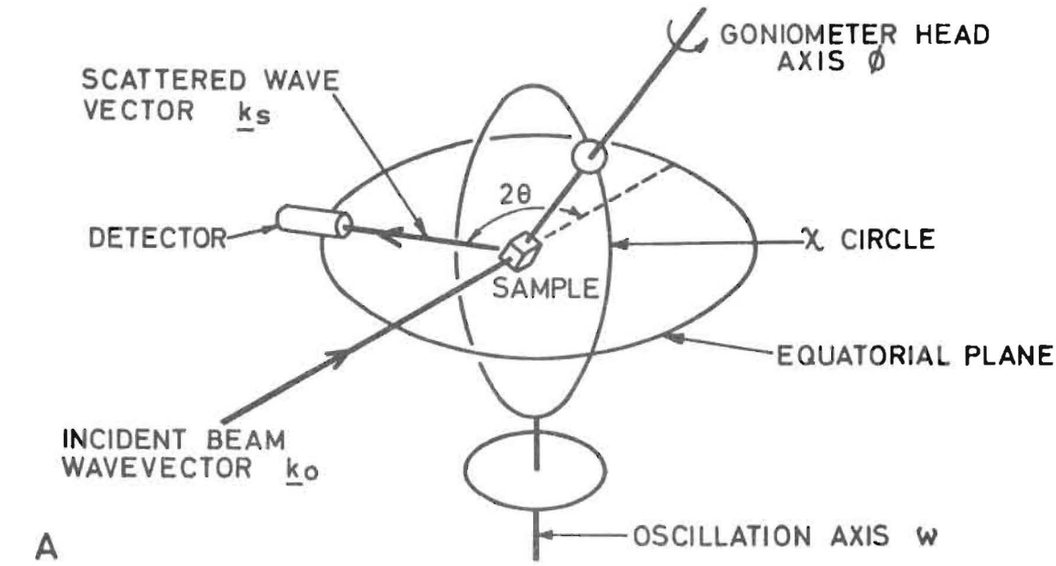

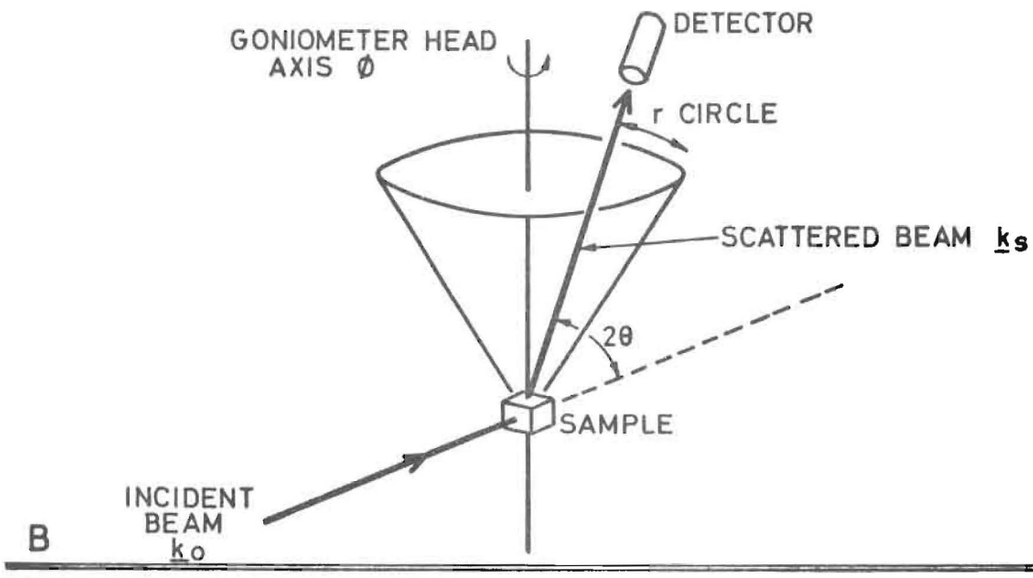

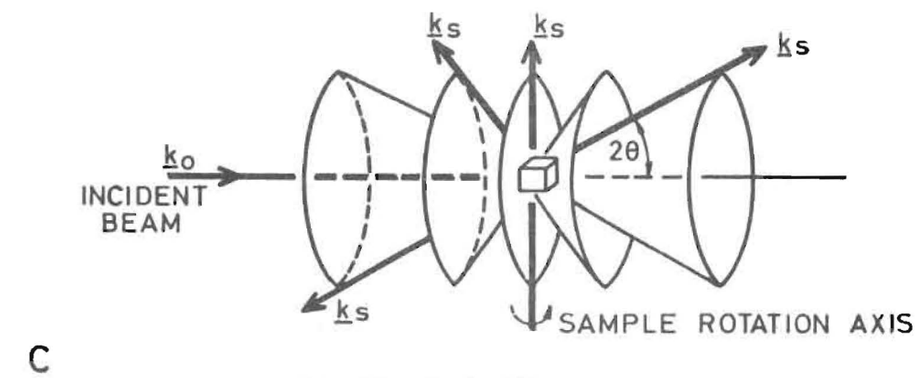

A. SINGLE CRYSTAL DETECTOR MOVING IN EQUATORIAL PLANE
B. SINGLE CRYSTAL DETECTOR ABLE TO MOVE AROUND AZIMUTHAL ANGLE
C. RANDOMLY ORIENTATED SCATTERER

Fig. 3. SCATTERING GEOMETRY

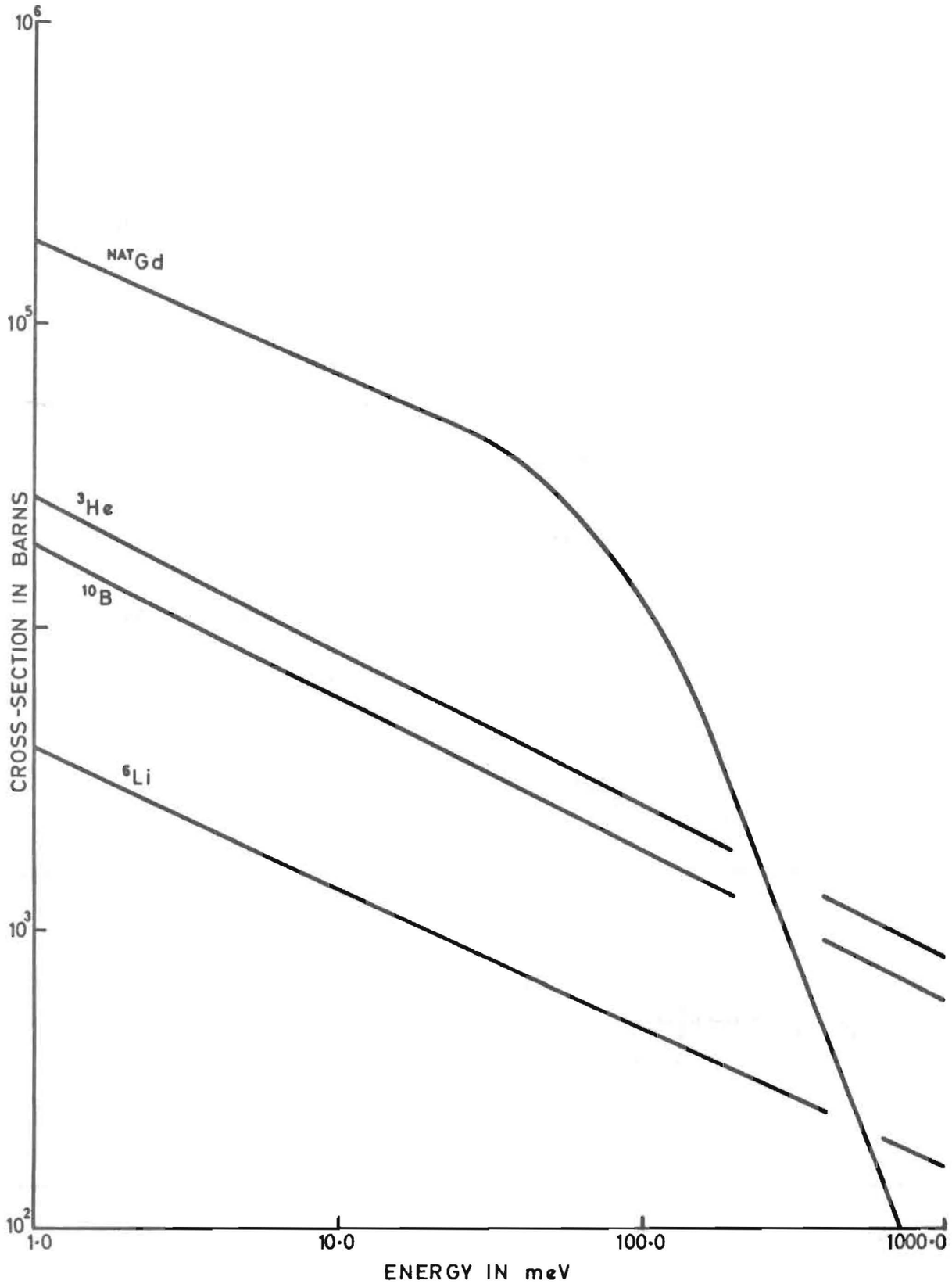

Fig. 4. TOTAL CROSS-SECTIONS

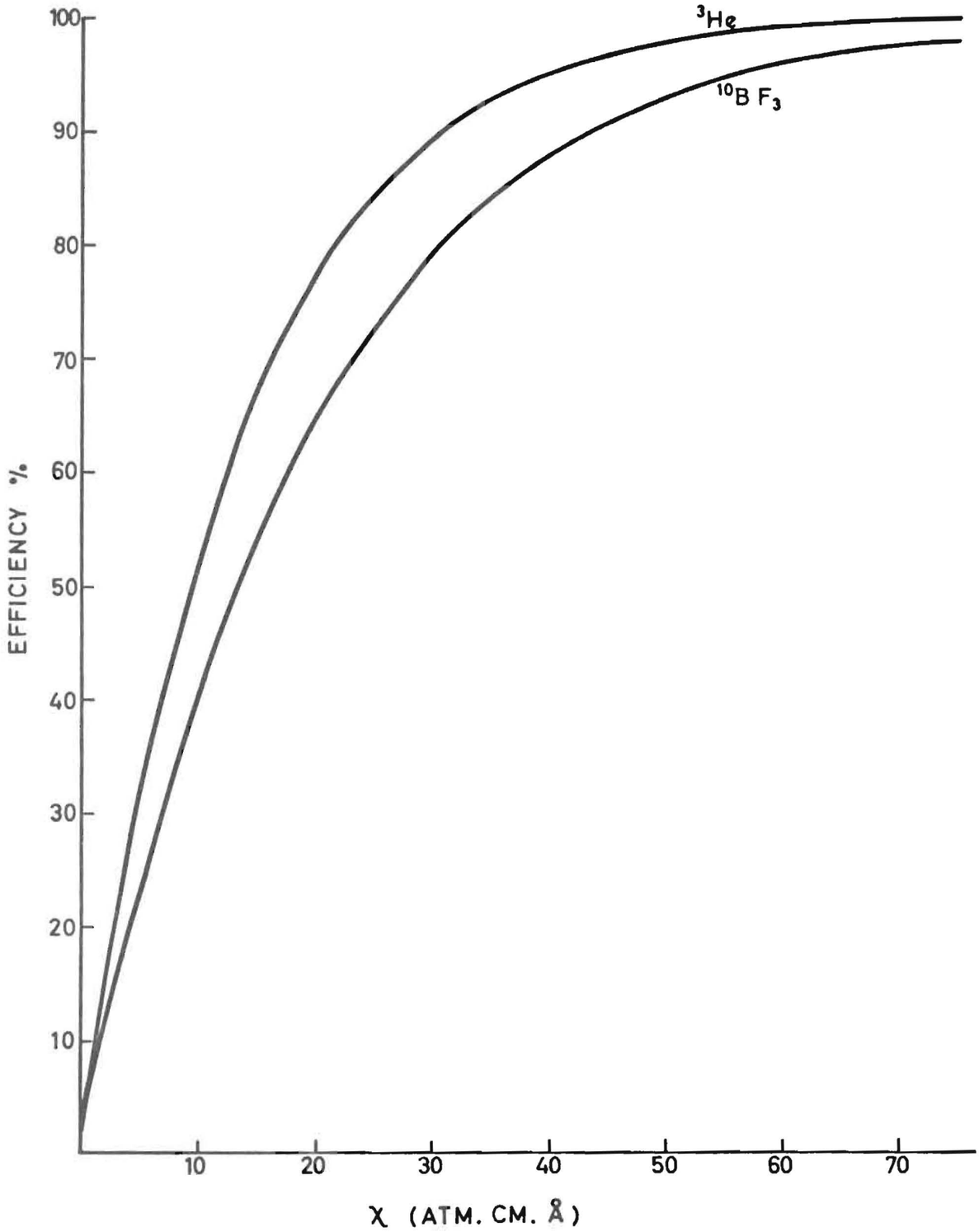

Fig. 5. GAS DETECTION EFFICIENCY AT 300°K

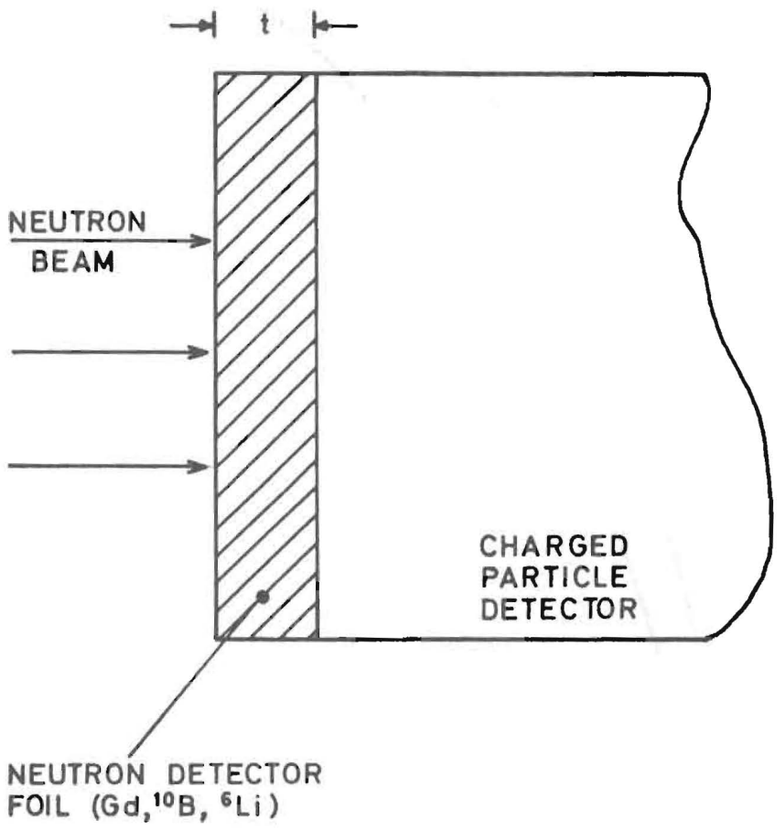

Fig. 6. FOIL GEOMETRY

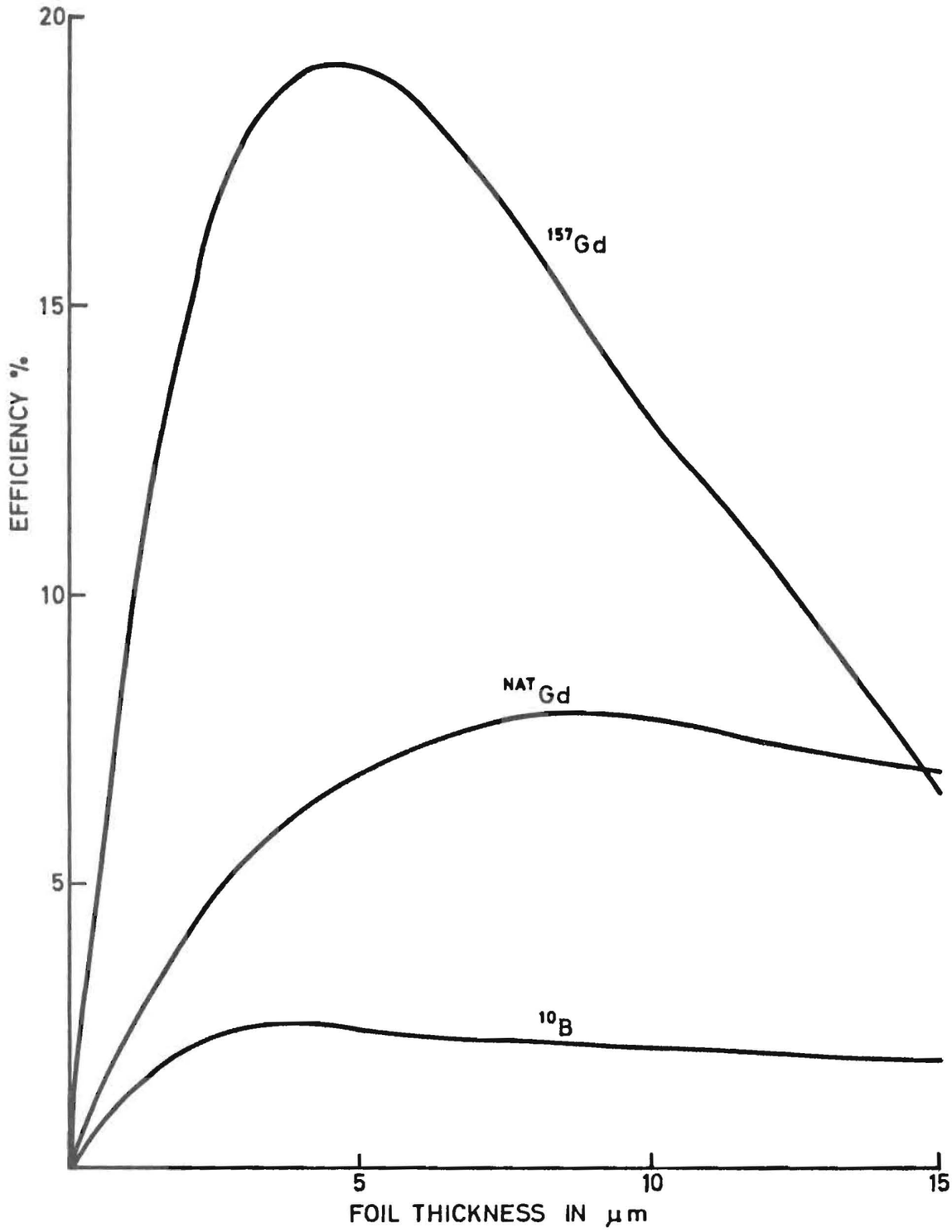

Fig. 7. FOIL EFFICIENCY

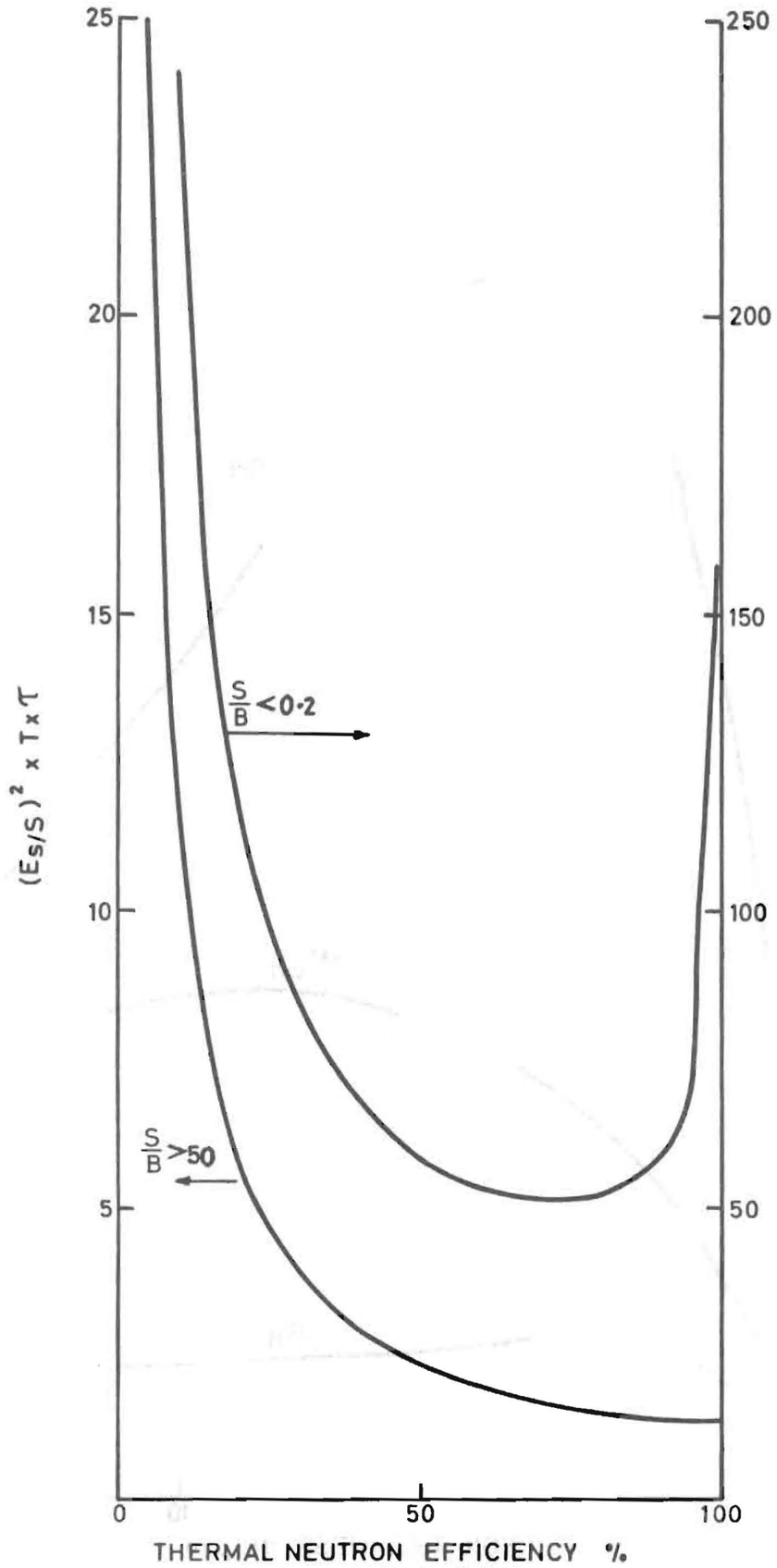

Fig. 8. DEPENDENCE OF FRACTIONAL ERROR ON EFFICIENCY

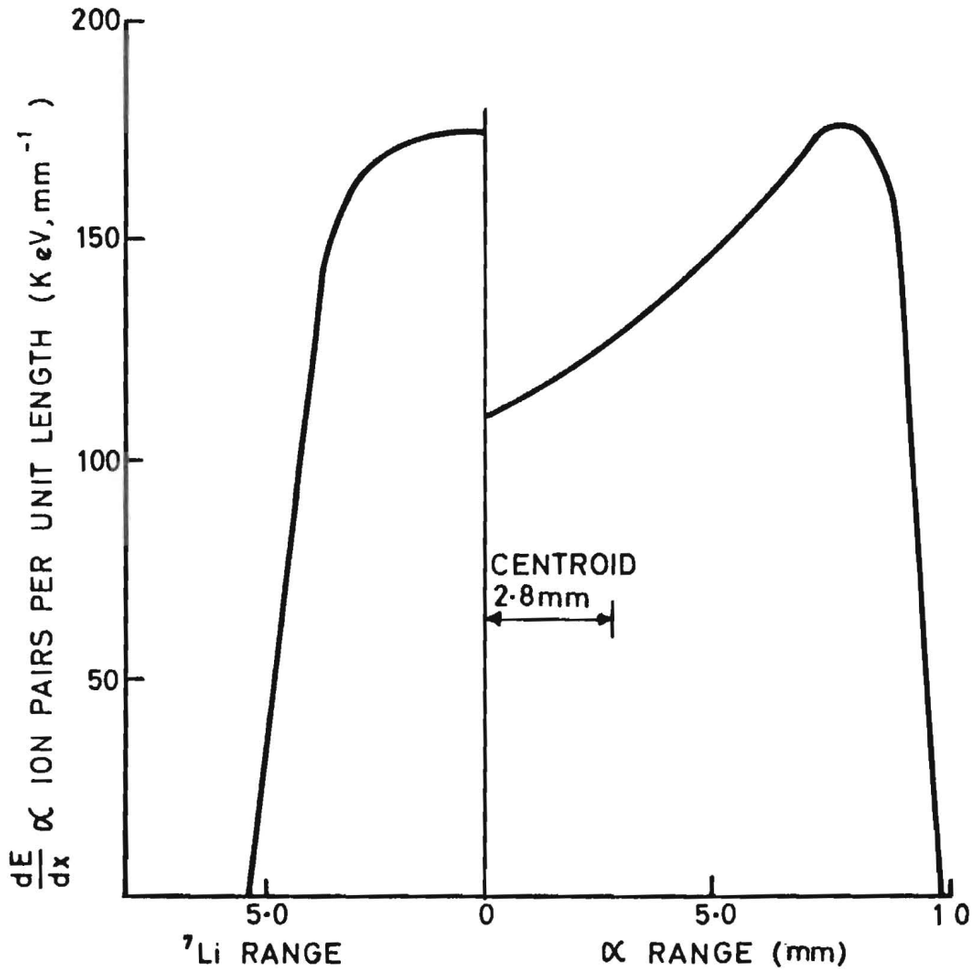

Fig. 9. CHARGE DENSITY FOR 1 ATM BF_3

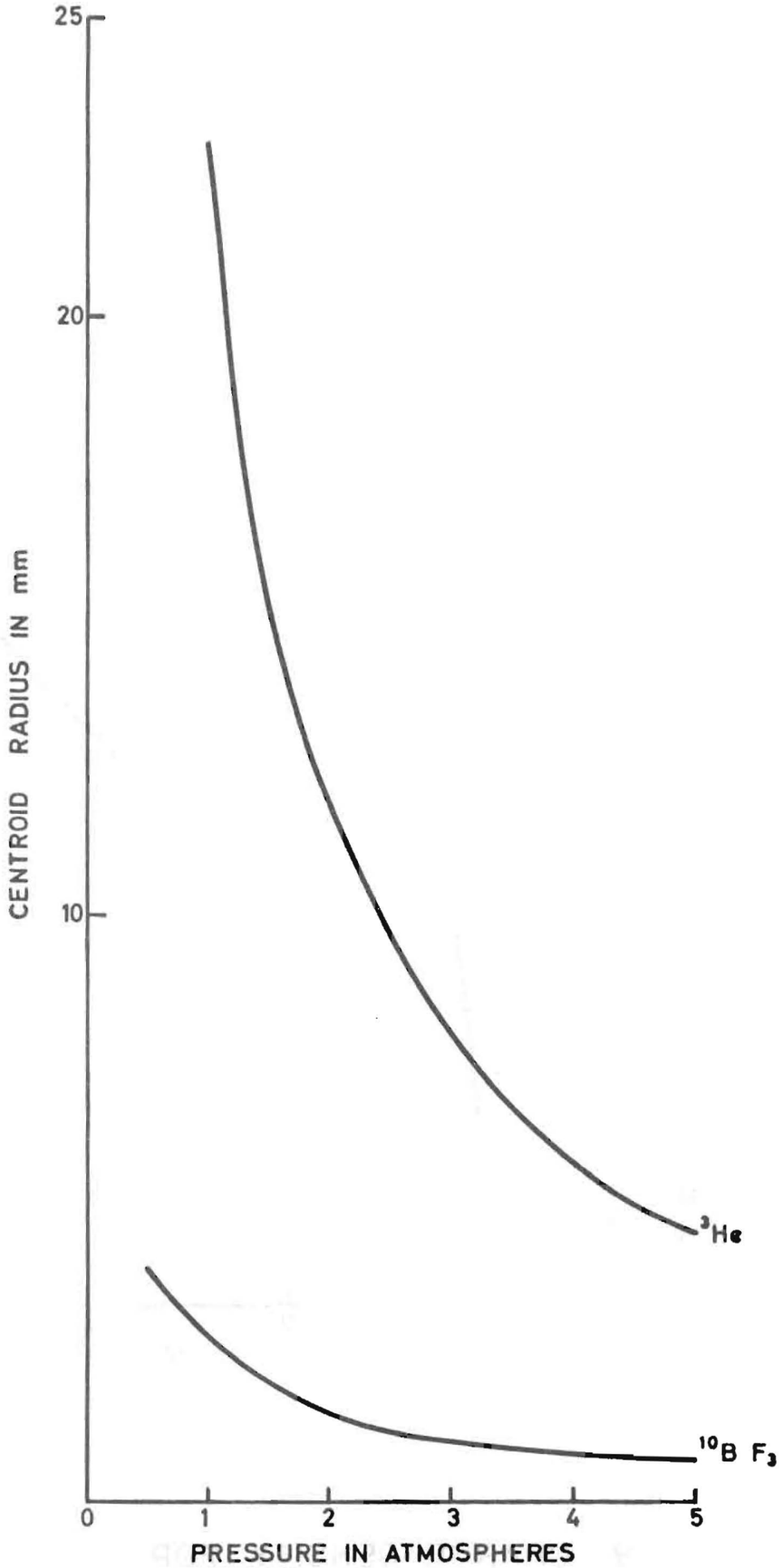

Fig.10. CENTROID RADII

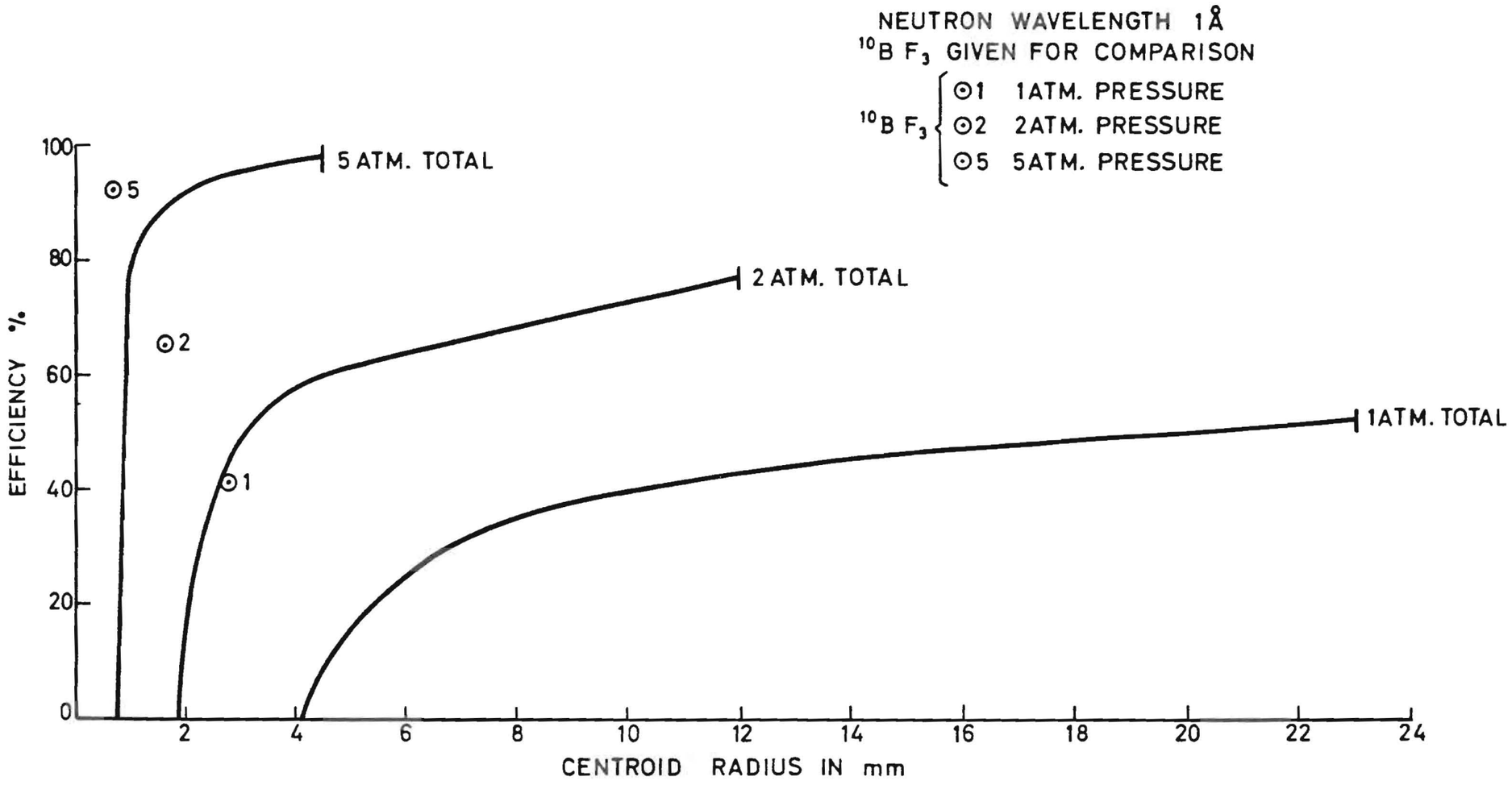

Fig. 11. EFFICIENCY / RESOLUTION FOR 10 cms. He/Kr MIXTURE FOR DIFFERENT TOTAL PRESSURES

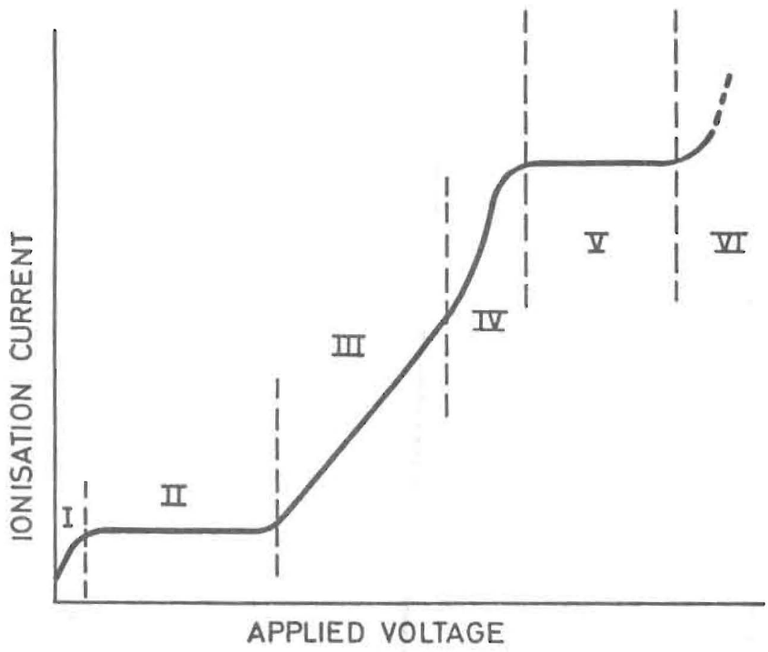

I INCREASING IONISATION
II IONISATION REGION
III PROPORTIONAL REGION
IV REGION OF LIMITED PROPORTIONALITY
V GEIGER REGION
VI SPARK REGION

IONISATION CURVE

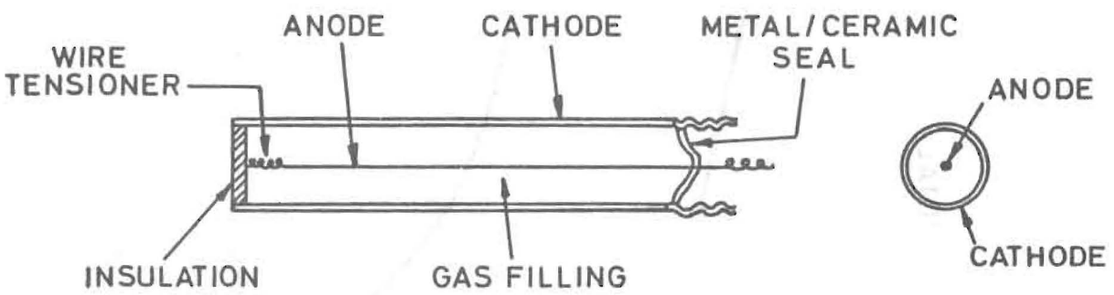

SIDE ELEVATION

END ELEVATION

A SIMPLE GAS COUNTER

Fig. 12.

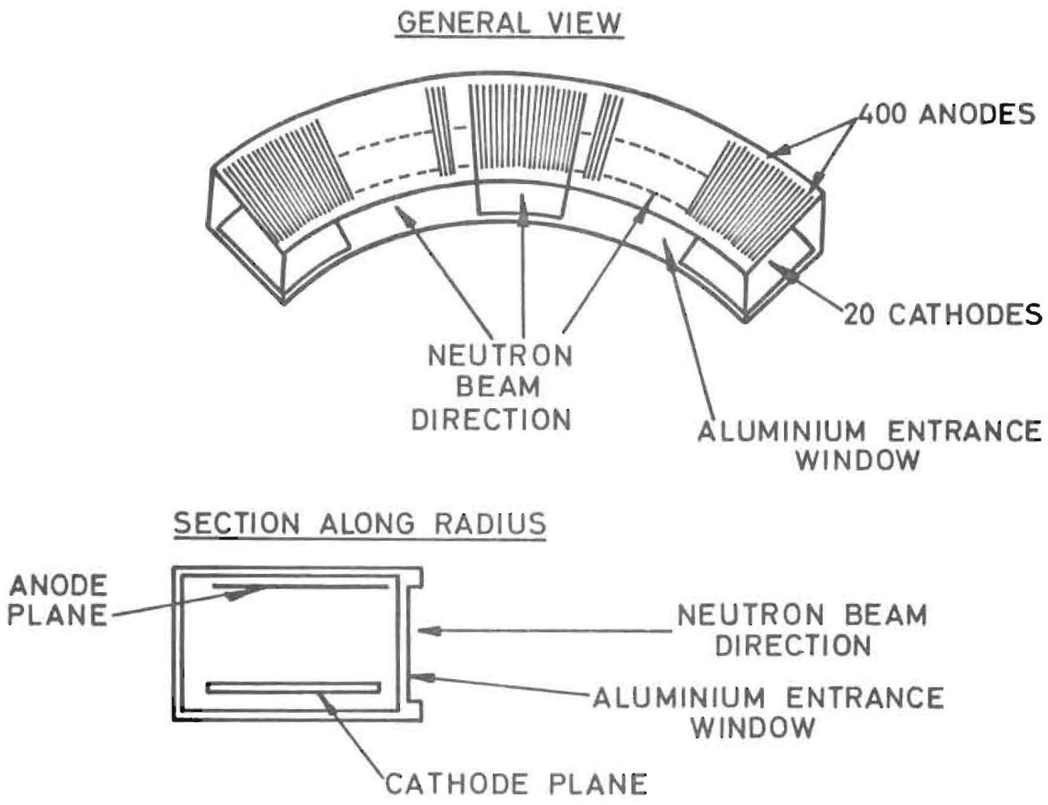

(i) ONE DIMENSIONAL DETECTOR

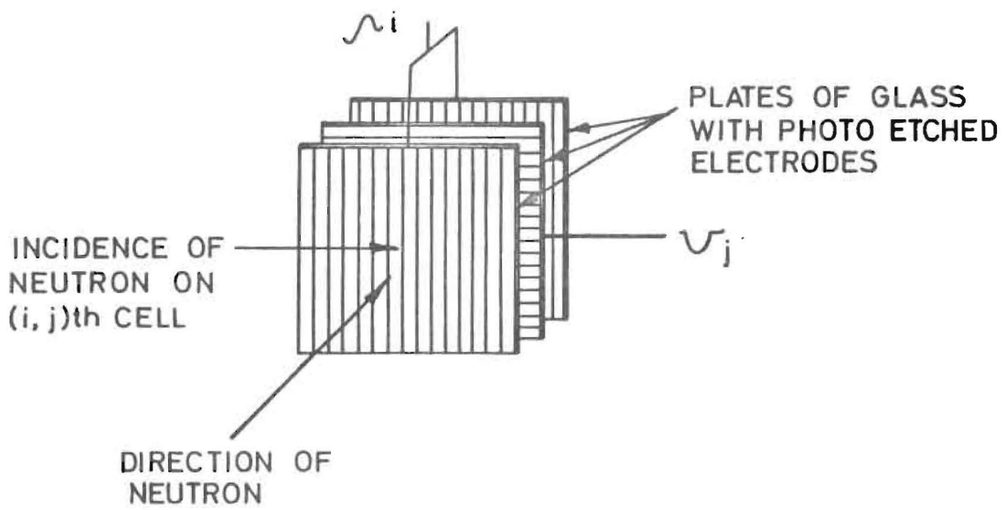

(ii) TWO DIMENSIONAL DETECTOR

Fig. 13. MULTI IONISATION CHAMBERS

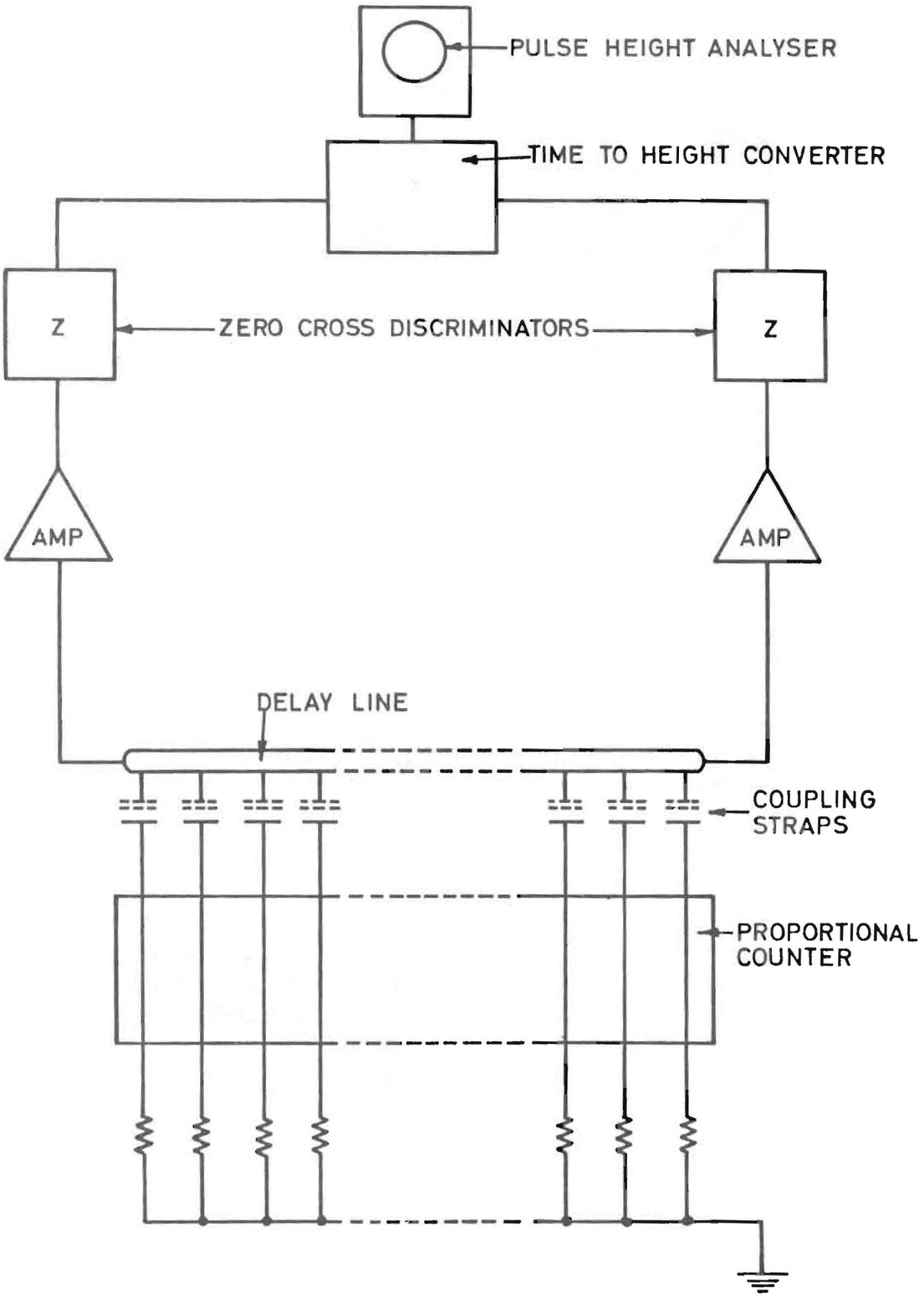

Fig. 14. DELAY LINE READ OUT

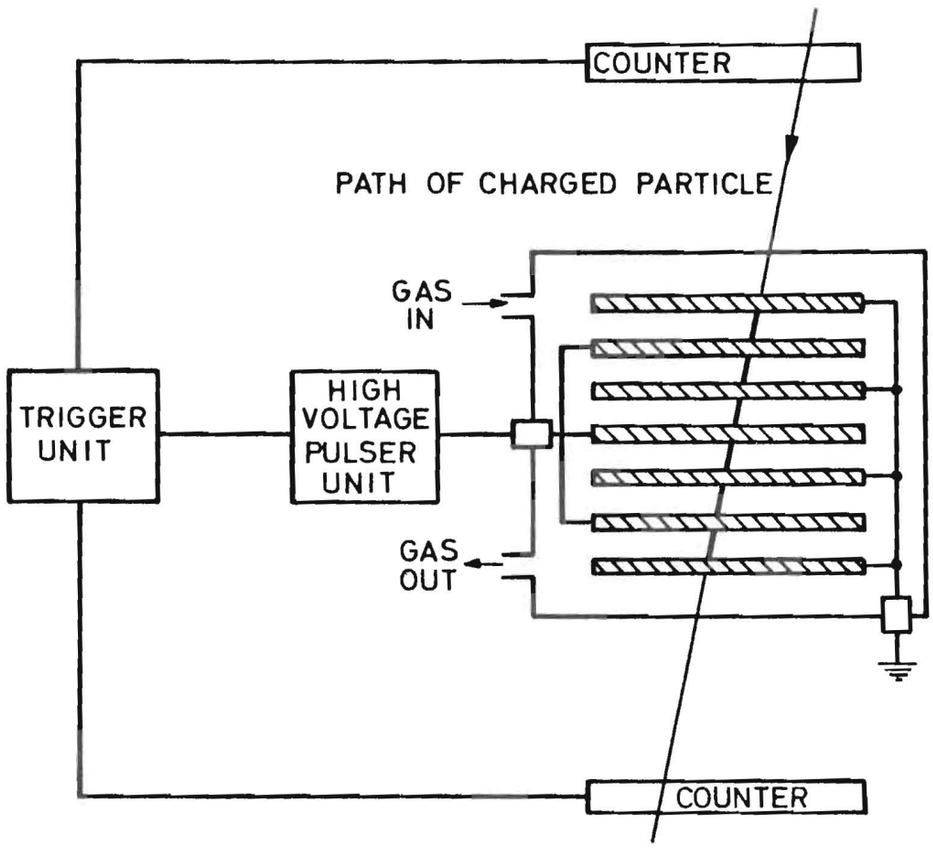

Fig.15. SPARK CHAMBER

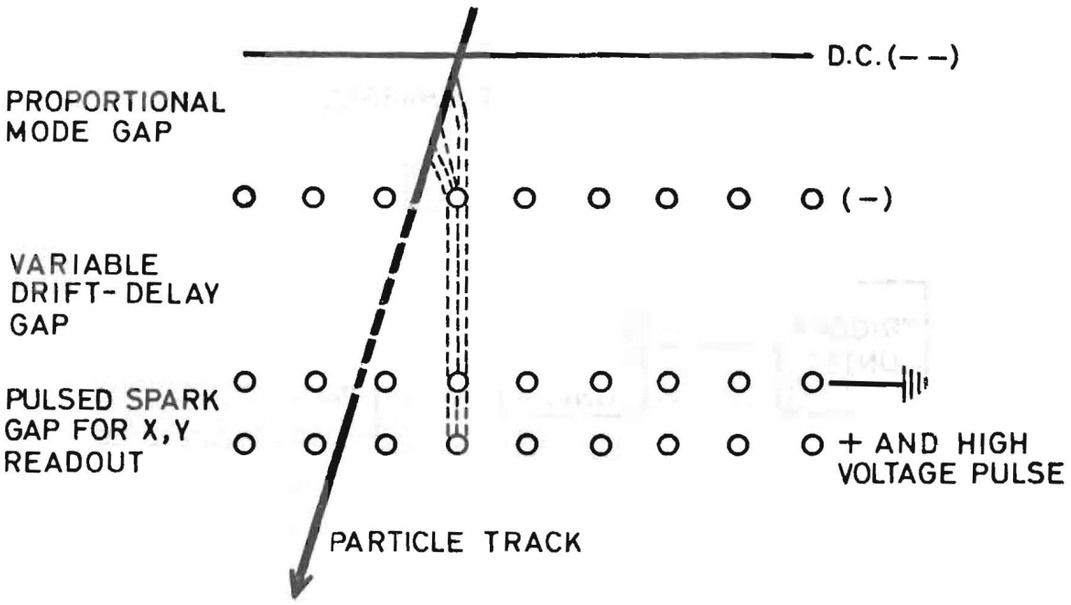

Fig. 16. HYBRID CHAMBER

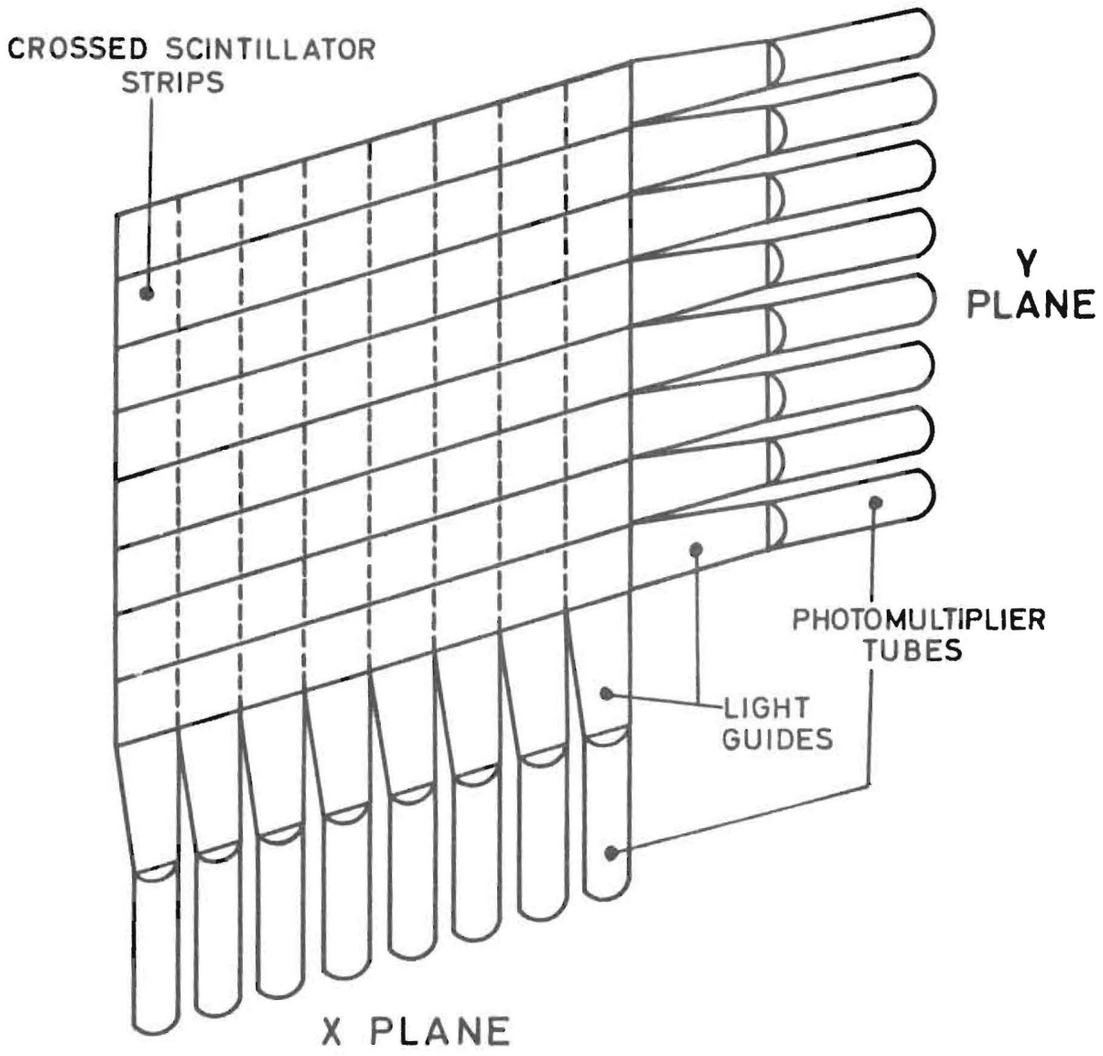

Fig. 17. SCINTILLATION COUNTER HODOSCOPE

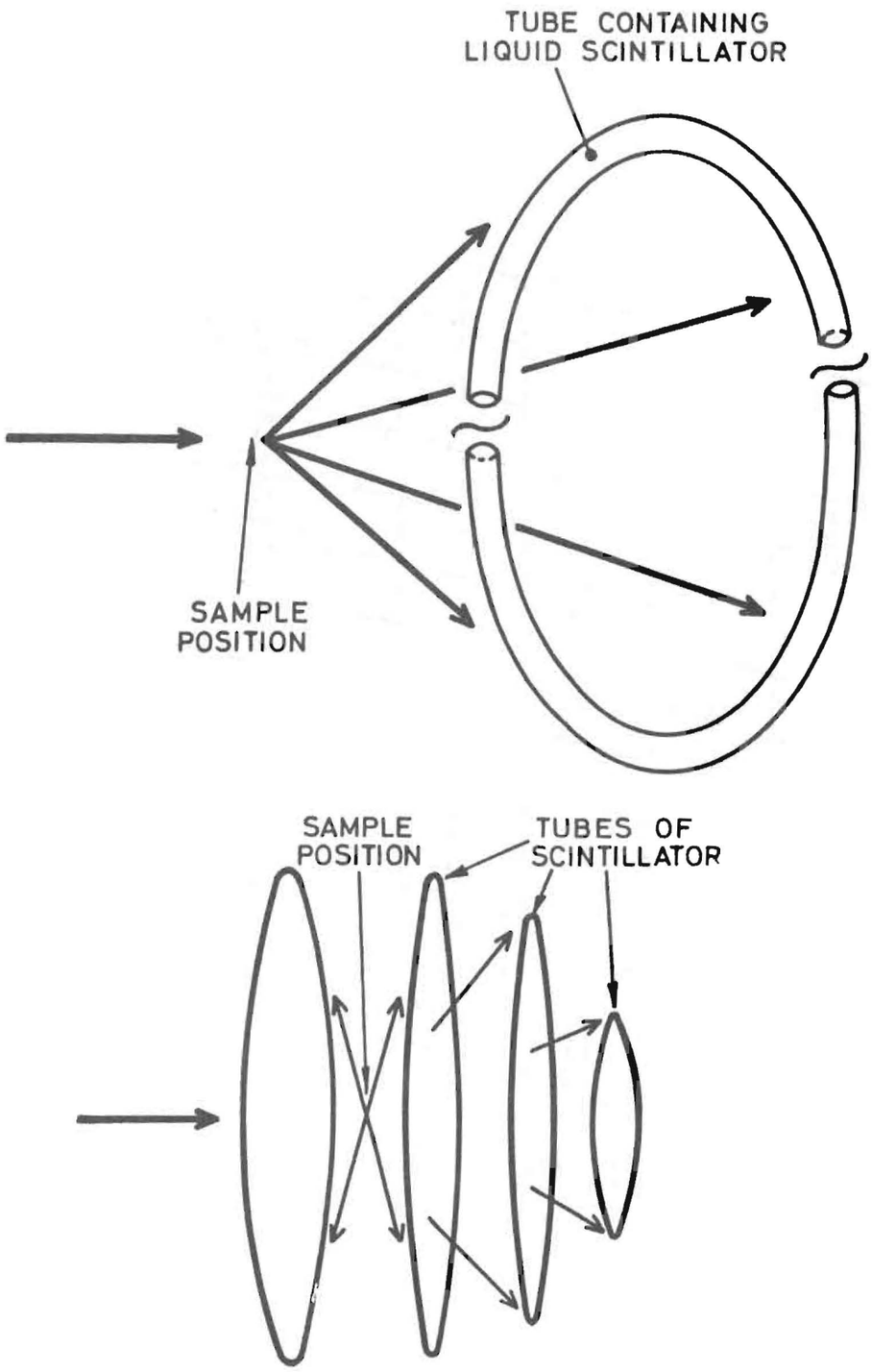

Fig. 18. ANNULAR RINGS OF LIQUID SCINTILLATOR FOR RANDOM SCATTER STUDIES

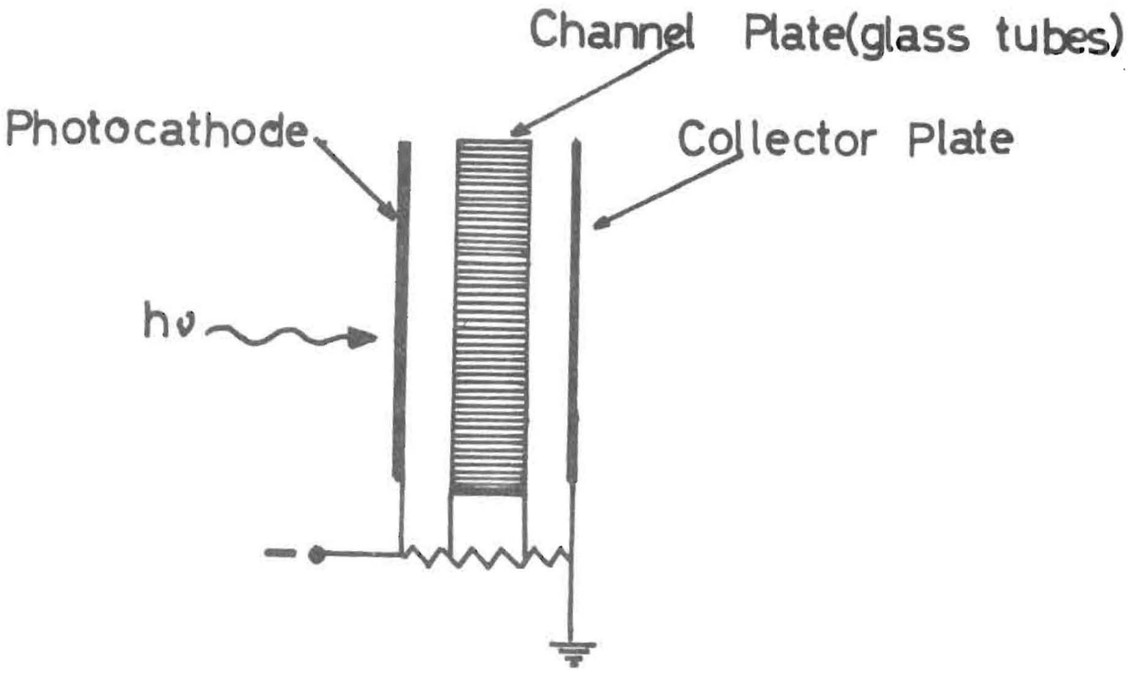

Fig. 19. PRINCIPLE OF CHANNEL PLATE.

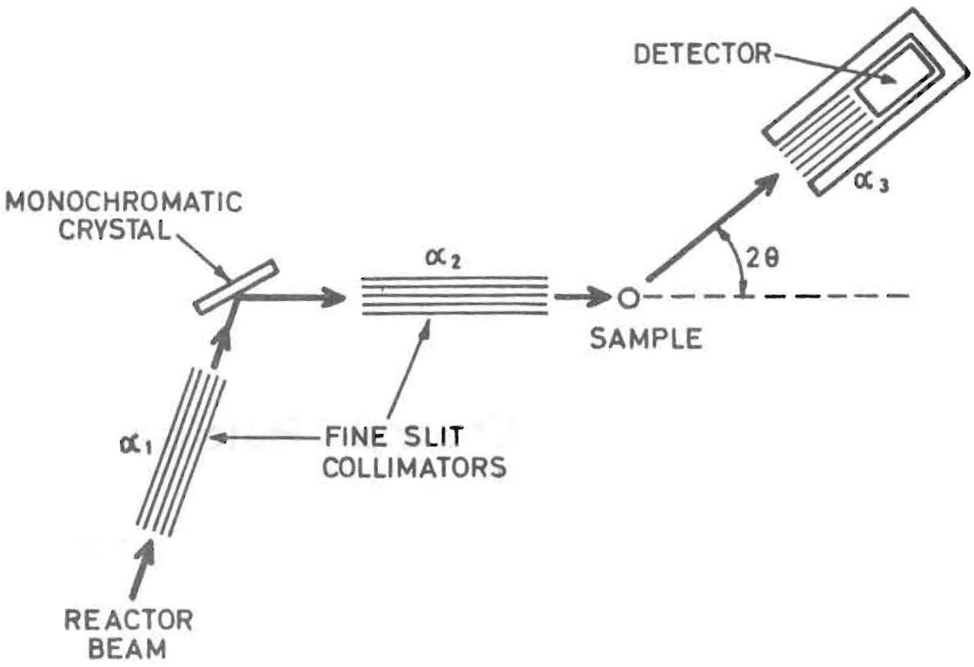

POWDER DIFFRACTOMETER

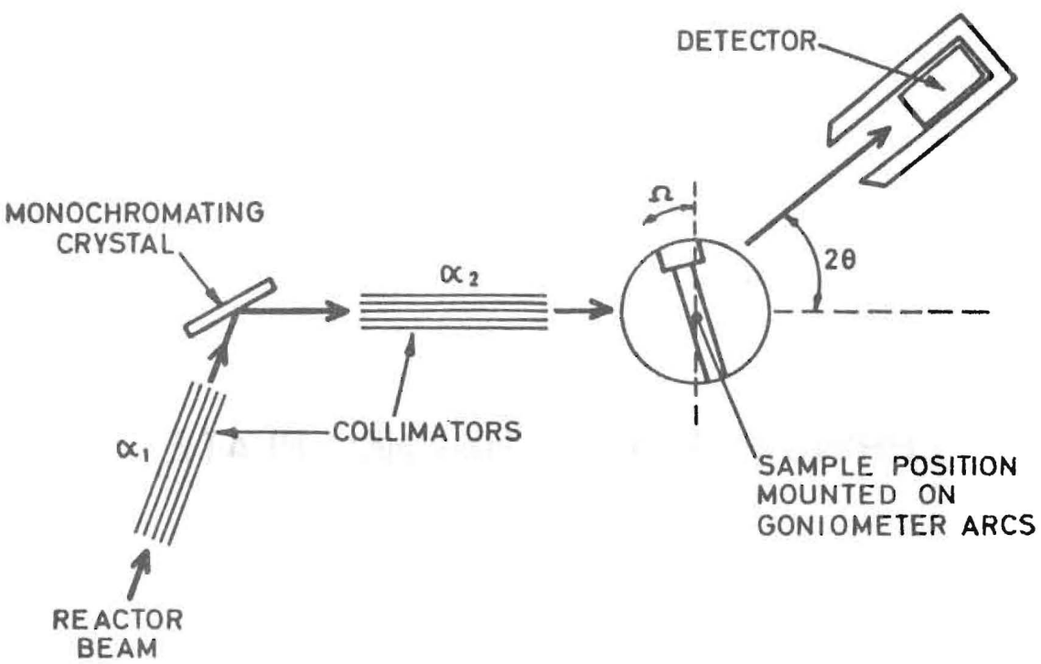

SINGLE CRYSTAL DIFFRACTOMETER

Fig. A1.

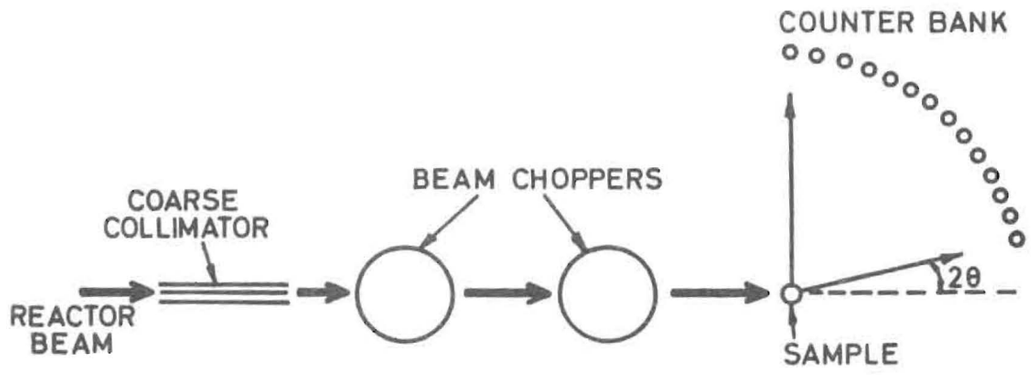

TIME OF FLIGHT INSTRUMENT

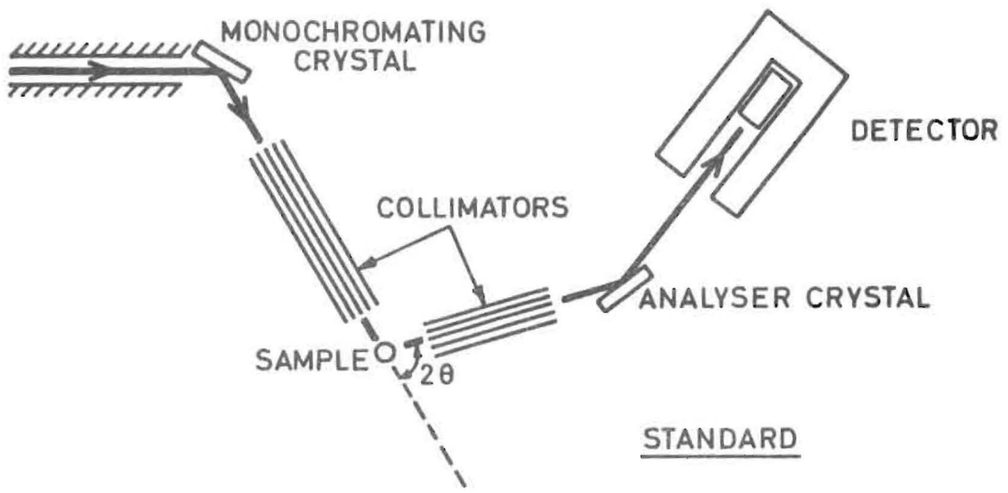

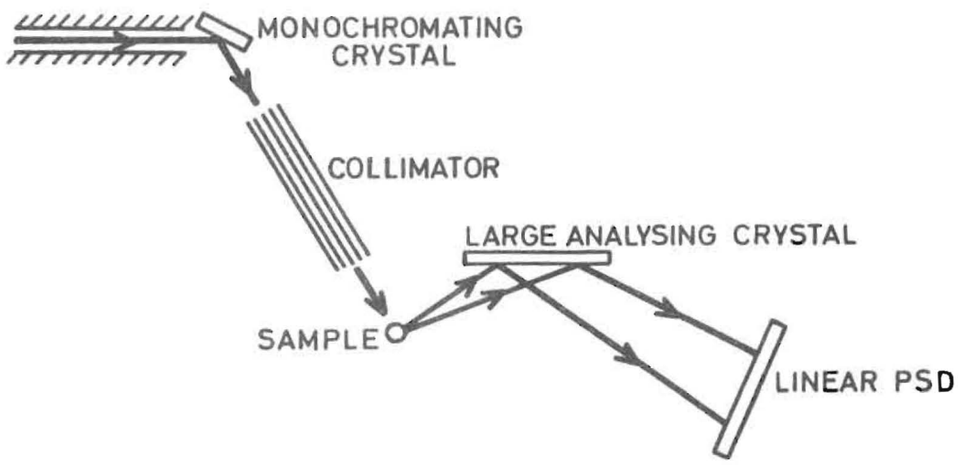

THREE AXIS INSTRUMENTS

Fig. A 2.

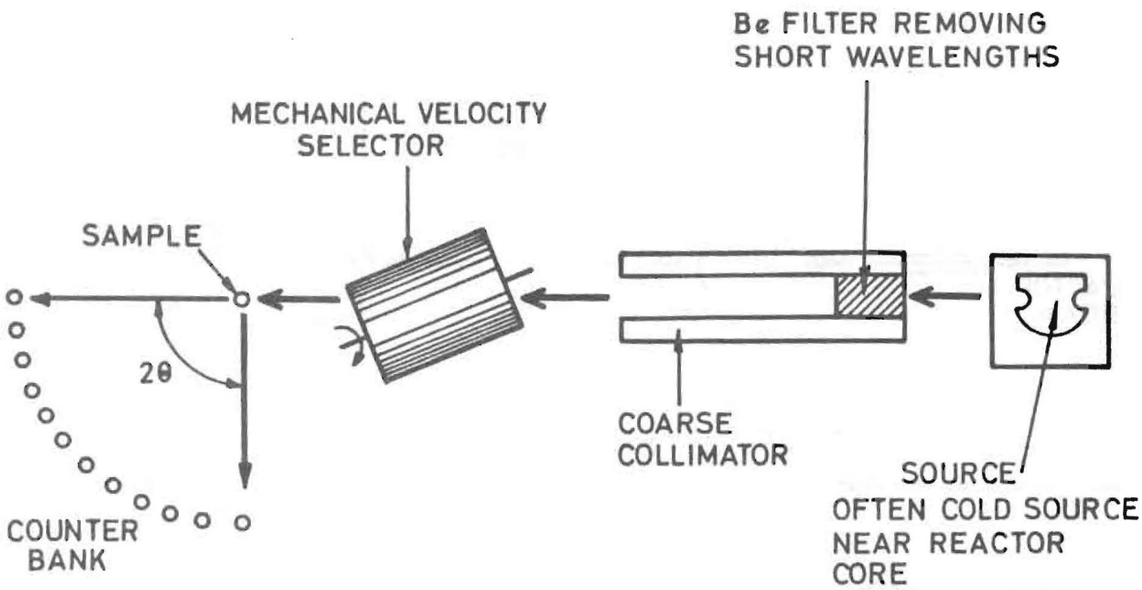

MONOENERGETIC DIFFUSE SCATTERING APPARATUS

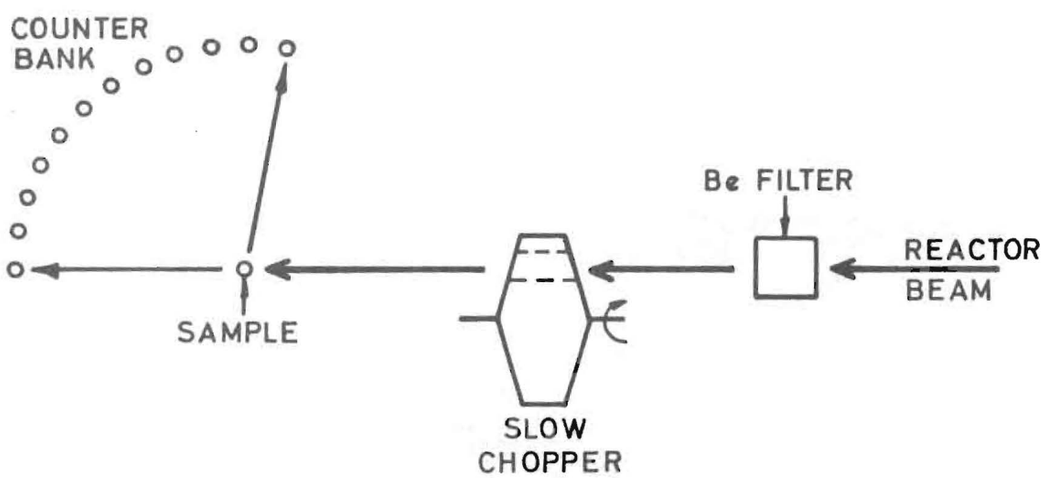

TIME OF FLIGHT DIFFUSE SCATTERING APPARATUS

Fig. A3.

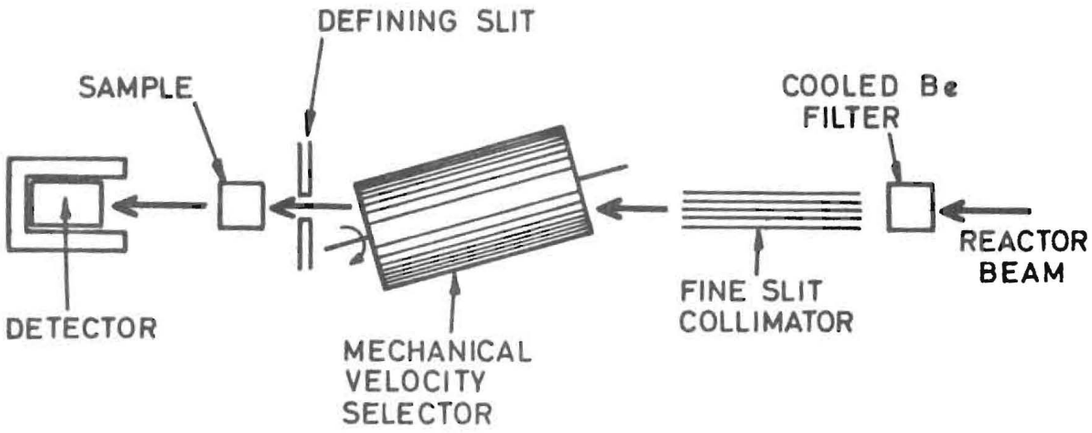

TRANSMISSION APPARATUS

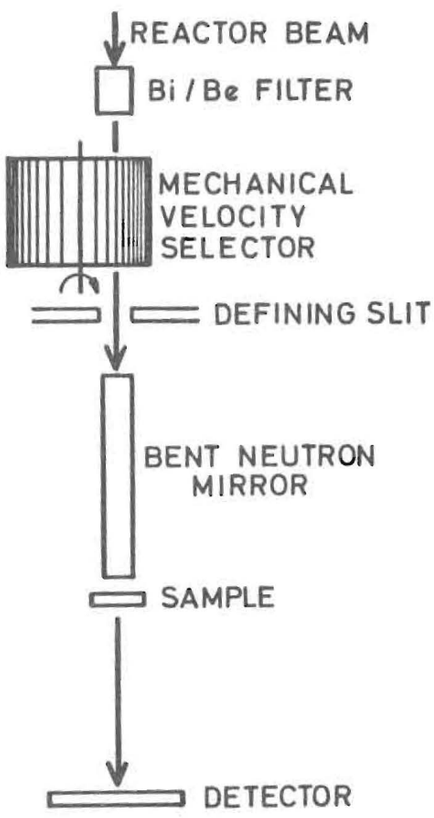

SMALL ANGLE SCATTERING APPARATUS

Fig. A4.